AD-A124 641 X-RAY SPECTROSCOPY TO DETERMINE LINE COINCIDENCES(U) 1/1
NAVAL RESEARCH LAB WASHINGTON DC P G BURKHALTER ET AL.
31 JAN 83 NRL-MR-5022

UNCLASSIFIED . F/G 20/5 NL

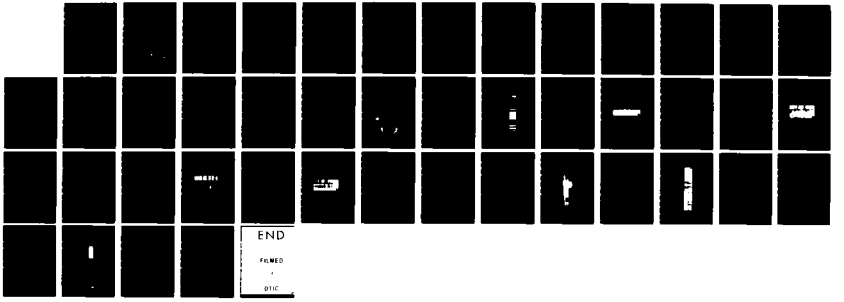

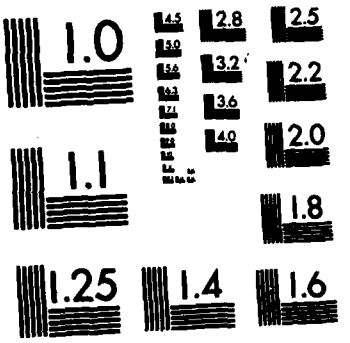

NRL Memorandum Report 5022

X-Ray Spectroscopy to Determine Line Coincidences

P. G. BURKHALTER

Condensed Matter Physics Branch
Condensed Matter & Radiation Sciences Division

G. CHARATIS AND P. ROCKETT

KMS Fusion, Inc.
Ann Arbor, MI 48106

January 31, 1983

This work was supported by the U.S. Department of Energy.

NAVAL RESEARCH LABORATORY
Washington, D.C.

SECURITY CLASSIFICATION OF THIS PAGE (When Data Entered)

REPORT DOCUMENTATION PAGE		READ INSTRUCTIONS BEFORE COMPLETING FORM
1. REPORT NUMBER NRL Memorandum Report 5022	2. GOVT ACCESSION NO. AD-AU4 641	3. RECIPIENT'S CATALOG NUMBER
4. TITLE (and Subtitle) X-RAY SPECTROSCOPY TO DETERMINE LINE COINCIDENCES		5. TYPE OF REPORT & PERIOD COVERED Interim report on a continuing NRL problem. 6. PERFORMING ORG. REPORT NUMBER
7. AUTHOR(s) P.G. Burkhalter, G. Charatis*, and P. Rockett*		8. CONTRACT OR GRANT NUMBER(s)
9. PERFORMING ORGANIZATION NAME AND ADDRESS Naval Research Laboratory Washington, DC 20375		10. PROGRAM ELEMENT, PROJECT, TASK AREA & WORK UNIT NUMBERS DOE 81201; RR012-02-41; 66-0859-B-2
11. CONTROLLING OFFICE NAME AND ADDRESS U.S. Department of Energy Washington, DC 20545		12. REPORT DATE January 31, 1983 13. NUMBER OF PAGES 43
14. MONITORING AGENCY NAME & ADDRESS(if different from Controlling Office)		15. SECURITY CLASS. (of this report) UNCLASSIFIED 15a. DECLASSIFICATION/DOWNGRADING SCHEDULE

16. DISTRIBUTION STATEMENT (of this Report)

Approved for public release; distribution unlimited.

17. DISTRIBUTION STATEMENT (of the abstract entered in Block 20, if different from Report)

18. SUPPLEMENTARY NOTES

*Present address: KMS Fusion, Inc., Ann Arbor, MI 48106

This work was supported by the U.S. Department of Energy.

19. KEY WORDS (Continue on reverse side if necessary and identify by block number)

X-ray spectroscopy
Plasma diagnostics
Lasing line coincidences

20. ABSTRACT (Continue on reverse side if necessary and identify by block number)

X-ray spectroscopy in the 12-15 Å region of L-shell lines from selected transition elements was performed in a joint Naval Research Laboratory — KMS Fusion, Inc. experiment. The accurate wavelengths determined in this work will be utilized in selecting potential pumping candidates in future X-ray lasing schemes. Specifically, high-resolution X-ray spectra were collected under controlled geometric and target

(Continues)

DD FORM 1 JAN 73 1473 EDITION OF 1 NOV 65 IS OBSOLETE
S/N 0102-014-6601

SECURITY CLASSIFICATION OF THIS PAGE (When Data Entered)

20. ABSTRACT (Continued)

conditions using both red and green light laser excitation in the KMS Chroma laser. Three groups of X-ray spectra were collected with highly-dispersive X-ray crystals at wavelengths centered at 12.543, 13.781 and 14.458 Å corresponding to He- and H-like lines from fluorine. Two specially-designed flat crystal spectrographs employing film shutters were used with pairs of beryl and TAP crystals. The spectra from potential lasant and pump candidates could be recorded on the same spectrogram to aid in identifying X-ray line coincidences. In cases where wavelengths were measured in both the red and green laser work, agreement within 1-3 mÅ was obtained for the L-series X-ray lines. Within this accuracy range, five L series X-ray lines, mostly 2p-3d transitions from the metals Cr, Mn, and Ni, had wavelength values coincident to K-series lines in fluorine.

CONTENTS

X-Ray Spectroscopy to Determine Line Coincidences

I. INTRODUCTION

One of the first experiments being planned for the new Novette laser at Lawrence Livermore National Laboratory in early 1983 is the resonant pumping of X-ray lines in the 10-15Å region.[1] Selected L-shell lines in transition metals will be used to pump K shell levels in Ne or F gas. The gas will be enclosed in a thin metal tube of the candidate element whose wavelength matches that of the lasant gas. The experiments are based on the theoretical study of the physics for a short wavelength laser design by P. L. Hagelstein.[2] A portion of his study was to search the literature to determine appropriate elements with intense transitions to match the proposed lasant lines. One seeks line pairs whose wavelength separations are within 0.1 eV which corresponds to knowing wavelengths within 1-2 mÅ in the 10-15Å region. In the past decade, a number of spectroscopic studies have been conducted using high temperature plasmas generated by focussed-laser beams and the vacuum spark source. Several groups, including those at Goddard, NRL, Culham, Lebedev, Rutherford, Soreq, Lund, and Racah, have performed spectroscopic X-ray studies to measure the wavelengths of L-shell transitions in metals. In a number of cases there has been duplication in the efforts to measure the wavelengths of some isoelectronic series such as the Ne-, F- and O-like transitions. Therefore one has some estimate of the accuracy that X-ray wavelengths can be measured by comparing wavelength values from the results of several laboratories. Upon examination of the measurements in search of pump candidates, many cases of wavelength uncertainties have arisen. Only in rare cases have the wavelengths agreed within 1-2 mÅ between two or more laboratories. Typically the accuracy quoted has been either 5 or 10 mÅ and this is generally the level of agreement in wavelengths. However, there are cases such as strong lines in Ne-like Ni where measurements have as much as 15 mÅ disagreement. Clearly, there existed a need to remeasure certain X-ray wavelengths under carefully-controlled experimental conditions with good spectral dispersion.

A number of metals were selected that would have possible spectral matches based on published wavelength data. The three wavelengths of interest in this current study correspond to the F He beta line at 14.458 Å, the F He gamma line at 13.781 Å and the F H beta line at 12.643 Å. The metals known to have transitions in these wavelength regions are Cr, Mn, Fe, Ni and possibily Co. In the 12-15 Å region, Fe spectra have been

Manuscript approved December 20, 1982.

most extensively measured and classified. Further identifications were necessary for the other elements, which required atomic structure calculations. The wavelengths of the fluorine lines are based on theoretical calculations [3,4] that are believed accurate to 1 mÅ. In the 14.458 Å region, values for F-like 2p-3d transitions in Fe have been reported by three laboratories.[5-7] For some of the stronger lines in Fe, the wavelength agreement is 1-2 mÅ among different laboratories. Therefore, these were used for calibration purposes and to determine the magnitude of the Doppler shifts in the F lines measured in the two flat-crystal spectrographs. At 13.78 Å there are not sufficient Fe lines to use for calibration. The wavelengths reported for Be-like Cr XXI were used; however, the agreement in wavelengths between two laboratories was only 8 mÅ.[8-9] In the 12.643 Å region there exist strong 2p-3s, 3d transitions in Ne-like Ni XIX. The values reported by various groups disagree by as much as 15 mÅ. Two intense Li-like Cr lines, the 2s-3p lines in Cr XXII, occur in this region. One finds that the values measured for these two lines at two different laboratories are nearly in agreement but are 7 to 9 mÅ higher than two independent theoretical studies.[10-13]

The L-series X-ray spectral patterns were collected in this work with higher resolution than has previously been reported. Previous studies used longer 2d spacing crystals such as mica or KAP. New spectral features were resolved in this study. A high precision in wavelength measurements was obtained because of the improved spectral dispersion in the back reflection region and the use of a comparator densitometer to measure line positions on the spectrograms.

The purpose of this report is to present wavelengths of lines measured as pumping candidates in transition metals. The accuracy of the wavelength determinations is dependent on the quality of the spectral data and the accuracy of the published or theoretical wavelengths used for calibration lines. The precision in measuring the X-ray lines was 1-2 mÅ in the best cases of distinct, narrow lines and 4-5 mÅ for the weaker or broad lines. The approach in the present work was to use calibration lines which appeared reasonable and compare the wavelengths obtained in the two sets of data collected the red (1.05μm) and green (0.53μm) laser light. Since the wavelength values were based on different sets of calibration wavelengths in the red and green laser light experiments, the degree of accuracy in this work could be ascertained. In cases where the calibration wavelengths are believed known to an accuracy of 1-3 mÅ, we have obtained that level of accuracy in the measurement of L-series X-ray lines.

II. EXPERIMENTAL

The high-powered Chroma laser was used in single-beam, f/6 illumination for experiments performed in the Special Experiments Laboratory at KMSF. A total of five spectrographs, an X-ray streak camera, two pinhole cameras, and filtered PIN diodes were used to record the X-ray emission from the plasmas produced by the focussing of the laser. The laser was focussed to match approximately to the size of the metal targets of 450 μm diameter. When used in the red wavelength, the laser delivered 80J and as a frequency-doubled green laser the energy on target was about one half this value. The laser pulselengths used in this study were either

100 or 200 psec duration. The laser intensity was 2.5 x 10^{14} W/cm^2 at 1.05 μm and 1.2 x 10^{14} W/cm^2 at 0.53 μm for 200 psec pulses. The focussing of the laser onto the target surface was important in order to achieve reproducible plasmas as viewed by the X-ray spectrographs. Figure 1 is a schematic of the alignment device used to reposition each target. An ancillary laser and a TV optical system were used to focus the target position before every shot. The reproducibility of the plasma position was monitored by the plasma images collected by the X-ray pinhole cameras. Two X-ray pinhole cameras viewed the target at 52° and at 90° to the laser beam axis. The 52° camera was filtered with 50 μm Be, and the 90° camera was filtered by 1 μm mylar and 1500Å Al. The pinhole camera at ϕ=90° was used to monitor the relative positions of the two or three plasma images collected for each element. The target positions were determined to be reproducible to within 100 μm on a shot-to-shot basis. In the case of metal targets, single shots were usually sufficient to record readable X-ray spectra with red light while two shots were required for the green light system. For fluorine targets, multiple shots were required. Depending on the transition, up to three shots were required to produce readable spectra. A set of K-edge filtered PIN diodes monitored the hard X-ray output of the laser-irradiated targets. The plasma temperature for generating the L-series spectra was determined to be 1 keV. The hard X-ray temperature varied from 16.5 keV for teflon targets to 12.5 keV for metal targets.

The targets were fabricated using two methods by the Division of Material Science at KMSF. The metal targets were evaporated through masks onto 3600Å parylene substrates and supported on Al frames with large 2 mm openings (see Figure 2). The metal targets used in the experiment were 450 μm in diameter and 600-700Å thick. The fluorine targets were prepared by spraying teflon particles onto the plastic substrate. The diameters of these targets were varied from roughly 250 to 600 μm. The shot-to-shot variations in target positions and target sizes were small enough not to affect the spectral patterns in most cases.

The spectrographs were placed in a one-meter diameter vacuum tank in selected angular positions and positioned about the target in a symmetrical manner as illustrated in Figure 3. Three spectrographs employed convex-curved KAP crystals and were used to collect survey spectra that provided information about the intensity and the degree of ionization for each shot. The two high-resolution spectrographs used pairs of flat crystals, either beryl (2d=15.95Å) or TAP (2d=25.76Å). Both types of diffracting crystals were selected because of their high reflectivities and high dispersion properties. The slits on the front of the spectrographs were positioned between 14 to 15 cm from the targets and the target-to-film distance for the flat-crystal spectrographs were roughly 40 cm depending on the wavelength being measured. The film positions were centered in the back-reflection regions of the spectrographs at 2θ Bragg angles of 120° (13.781Å), 129° (14.458Å) and 158° (12.643Å). The flat crystal spectrographs had photographic film shutters positioned in front of the X-ray films that

allowed recording two to four spectral traces on each shot series. A movable shutter with a 6mm opening was placed in front of the film and repositioned between elements. Spectrograms with a variable amount of spectral overlap were acquired. The traces were about 4 cm in length using the beryl crystals and about 7 cm in length with the longer TAP crystals. The traces were collected physically adjacent or overlapping in order to obtain accuracy in wavelength determinations and to observe the line coincidences. The windows of the spectrograph were aluminized polypropylene stretched to a thickness of 0.85 μm. In front of each spectrograph, a debris shield of stretched polypropylene was used to protect the light-tight entrance windows.

The method for collecting data involved several steps. First, a target was positioned with the secondary laser beam and focussed with the TV monitor. The spectrographs were loaded with film and the shutters were set after positioning in the target chamber. Following a shot, the survey spectrographs were removed and films developed. The flat-crystal spectrographs were not moved during a series of shots. Following a recording of acceptable survey spectra, the shutters were repositioned on the flat crystal spectrographs and another target was positioned. With red light a single shot on the metal targets often provided usable spectra. The fluorine lines required 3 shots of 200 psec pulse duration to obtain sufficient line intensity. With green light only metal targets were used. Two shots per element were required to collect readable X-ray intensities because the available laser energy was less. The recording of a suitable spectrogram generally required a full day of between 6 and 8 shots. Each spectral series at a selected wavelength was collected at two different angular positions with the pair of diffraction crystals. Each spectral series was repeated to insure spectral reproducibility. The wavelengths used for calibration were the fluorine lines and published wavelengths for Fe and Cr lines. The wavelengths for the potential pump lines of interest were determined from two separate experiments. In the red light series, the fluorine lines were used for calibration after correcting for Doppler shifts. In the green light series, published Fe and Cr wavelengths were used for the 120° and 129° settings using the beryl crystals. Both experimental and theoretical values were employed for Li-like Cr lines in the 158° setting employing second-order TAP crystals.

The X-ray line positions were measured and spectral patterns recorded with two separate Grant densitometers. The line positions were read on a comparator incorporating a split image system. The positions of the spectral line patterns of metal and of the fluorine calibration lines could each be set independently and read alternately by simply rotating the prism. Selected spectrograms read with the Grant comparator densitometer were calibrated with a least-square polynomial program. A precision of 1-2 mÅ was determined obtainable for the intense, distinct lines from a comparison of wavelengths read from the two spectrographs. The line positions of broad, weak or overlapping lines were more difficult to determine accurately.

Spectral patterns were also processed by scanning with a digitizing Grant densitometer. Digital readings were recorded at every 10 micron intervals across the spectral patterns which were 4 to 7 cm wide. The digital readings were stored on magnetic tape with a PDP-8 computer and processed with a computer program that converts film densities to spectral intensities[14] in the NRL Advanced Scientific Computer. The spectral densities were converted into relative X-ray intensities with known calibration data for SB-5 film[15] and theoretical crystal reflectivities for Beryl crystals[16] and calculated values for second order TAP.[17] The data for rocking curves for the diffraction crystals was published by Burek.[18] The spectral traces were used to compare with theoretical calculations using the Cowan atomic structure program[19] in order to subsequently interpret newly-observed transitions such as in Be- and B-like Cr and Mn and the Na- and Mg-like satellite lines in Ni.

The design of the X-ray crystal spectrographs was dictated by the desirability to acquire high-dispersive spectra from a series of elements on the same spectrogram. A search was made to find suitable diffraction crystals to diffract 12-15 Å wavelengths in the backreflection region of the spectrographs. Only a few X-ray diffraction crystals have 2d spacings in this region. Acid phthalates crystals with d spacings of about 13 Å can be used in second-order reflection. TAP with a d spacing of 12.88 Å is a good choice for spectral measurements 12.643 Å which corresponds to the H beta line in fluorine. TAP has good reflectivity with R values of about 10^{-4} rad in second order; however, the rocking curve for TAP is unknown in second order. A value was estimated from the calculated rocking curve value for second order in KAP[18] and from a comparison of first order rocking curves for KAP and TAP. The rocking curve value estimated for second-order TAP was 3.2 arc min at 12 Å.

Only two naturally-occurring diffraction crystals are known to have 2d spacings of about 15-16 Å. Gypsum is one; however, its reflectivity is low and gypsum deteriorates under vacuum. Beryl has a 2d spacing of 15.95 Å and high reflectivity with R values of 10^{-4} rad in the back reflection region. For highly-polished and etched beryl crystals, a rocking curve of 3.3 arc min has been reported for Cu L radiation.[16] The group at the Rutherford Laboratory has been using beryl for collecting X-ray data in orbiting satellites. Fortunately, we were able to acquire on loan a pair of beryl crystals to use in this work. The beryl crystals diffract wavelengths in the 13-15 Å region at high 2θ values.

III. RESULTS

The spectrograms for the red light experiments contained metal spectra and Doppler-shifted F lines to observe relative line positions of lasant and potential pump lines. The spectrograms in the green light experiments contained two or three metal spectra that overlapped in position sufficiently to provide accurate wavelength calibration. The wavelengths of the lines determined in the two sets of experiments were compared in order to arrive at final wavelength values. Potential pump lines were determined from the wavelength values where line coincidences were found. We will first examine selected spectrograms from the two experiments and interpret the spectral scans. From a tabulation of the measured wavelengths, line matches can be selected.

A. 14.458 Å region

The pair of beryl crystals were mounted in the flat-crystal spectrographs at angles corresponding to Bragg 2θ values of 129° for the 14.458 Å lines of fluorine. Figure 4 shows the spectrogram recorded at 129° for F and Cr. The F He beta line required three shots with red light to record while the Cr lines were recorded in two shots. The position of the F He beta line has been Doppler shifted to 14.464 Å. The F line occurs in a spectral region with strong B-like Cr XX lines. The wavelength for F He beta at 14.458 Å occurs between two intense Cr lines and is coincident with a weaker line that can better be seen from densitometer scans. The F lines have broad, asymmetric profiles due to Doppler shifts over a distribution of ion velocities while the X-ray lines from the metal targets are nearly symmetric. The resolving power, $\lambda/\Delta\lambda$, using the beryl crystals is determined from the single-shot metal spectum to be 1700. The densitometer trace acquired from the spectrograph at Ø equal to 126° for Cr and F is shown in Figure 5. The asymmetric F line is shifted as indicated. The Cr line at 14.458 Å is in coincidence with F He beta.

Several spectrograms were recorded and calibrated to determine the Fe and Doppler-shifted F wavelengths. Fluorine-like Fe lines have been measured by three groups, namely, Feldman, et al at NRL,[6] Gordon, et al at Culham[5], and Boiko, et al at Lebedev.[7] A wavelength agreement of 1-2 mÅ was found for nine strong Fe XVIII lines and poorer agreement existed in the comparison for the weaker lines in the three reported measurements. For the spectrograph set at Ø equal to 180° from the incident laser beam, the F lines had peak positions that were +6 to +8 mÅ higher than the 14.458 Å value for the F He beta line. The spectrograph viewed the target from the rear at an angle of 30° from the beam. The plasma is seen by this spectragraph as a column with a velocity distribution directed as a cone towards the laser, which yields a positive wavelength shift. This is consistent with the ion velocity distributions with maximum ion velocities in a cone directed towards the laser axis as deduced from the spatial and temporal data collected from laser produced carbon plasma by Irons, et al.[20] The measured peak line shifts for the F He beta line relative to the iron spectral lines corresponds to ion velocities between 1.2-1.8 X 10^7 cm/sec. The measured shifts in the F He beta line for the spectrograph positioned at 126° with respect to the laser beam were 3-4 mÅ, which are consistent with calculated shifts of 3.5-4.7 mÅ for the velocity distributions determined from the 180° data. The Fe lines were measured and compared for the spectrogram collected at 180° and 126°. The wavelengths of the Fe lines near 14.458 Å from the two spectrographs were determined to be equal within 1-2 mÅ, indicating smaller ion velocities for the metal targets than for fluorine targets. In the green light study, the 126° spectrograph was repositioned to 105° from the incident laser beam to further reduce the Doppler shifts in the data. The wavelengths determined in the green light work from the transition metals are based on the assumption that the relative ion velocity distributions produce negligible Doppler shifts. The difference in ion mass between F and Fe particles is about 13 percent. The line profiles were generally sharper for the spectra collected nearer to the normal of the laser beam. Spectral emission was not observable with the spectro-

graph positioned at 90° to the laser beam because the target holder blocked the plasma emission.

The spectrogram for F and Fe spectra is shown in Figure 6. The Doppler-shifted F He beta line is overlapped with weak 2p-3d transitions from F-like Fe XVIII. Figure 7 shows the densitometer trace for the F He beta line and the Fe XVIII spectral region. The identification of the $2p^5-2p^4 3d$ transitions in Fe XVIII could be made from the overlap of atomic structure calculations with the intensity traces shown in Figure 8. The wavelength region where the F He beta line aligns with the Fe spectrum has several weaker transitions in Fe XVIII.

With the green light laser, spectra were recorded for Cr, Fe and Mn targets. The spectrogram for these three elements is shown in Figure 9. The relative intensity scans for these three elements are shown in Figure 10. The wavelength position corresponding to the F line at 14.458 Å aligns with a weak Cr line and a Mn line. Atomic structure calculations were performed for B-like Cr XX and Be-like Cr XXI transitions. At a wavelength of 14.458 Å the lines are solely from B-like Cr and the atomic structure calculations are shown overlapped in Figure 11. Atomic structure calculations for $2p^3-2p^2 3d$ transitions in N-like Mn XIX yields lines for this spectral region, as seen in Figure 12. The line coincident with the F line may belong to these transitions but a detailed analysis is needed.

B. 13.781 Å region

The pair of beryl crystals and the film holders were respositioned to collect spectral data at a 2θ Bragg angle of 120°. Spectrograms contained recorded emissions from F, Cr, and Ni plasmas. Upon examination of the spectrogram produced by red light and shown in Figure 13, one finds that both the Doppler-shifted F He gamma and delta lines align with lines in the Ni spectrum. The shifted F He gamma line is about +14 mÅ from an intense Cr line. The Doppler-shifted F He delta line aligns with a Cr line within 0.1 mm. The dispersion of this spectral region is 0.021 Å/mm. The densitometer traces for the F, Cr, and Ni spectra are shown in Figure 14. The strong line in the Ni spectrum is a 2p-3d transition in Ne-like Ni XIX.

The green light laser produced spectra for Cr, Mn, and Fe targets and the spectrogram is shown in Figure 15. This spectrogram was read and calibrated to determine line matches and to compare with spectra measured using the Doppler-corrected F line wavelengths. For the Cr line at 13.774 Å near the F He gamma line, the wavelength agreement between the red and green experiments was 1-2 mÅ. The Ni and Cr lines were found to differ by ±7 mÅ from the F line while the Mn line measured as a shoulder to an intense Mn line was -4 mÅ from the He gamma line. A Cr line was found that had a wavelength +5 mÅ from the value for F He delta line. The relative intensity trace for the Cr, Mn Fe spectra centered around 13.781 Å is shown in Figure 16. Atomic structure calculations for Cr XX and XXI reveal that lines in the 13-14 Å region belong mostly to Be-like Cr XXI. Figure 17 shows the Cr XXI calculations in this spectral region.

Atomic structure calculations were performed for Be- and B-like Mn XXII and XXI 2p-3d transitions. The predicted spectra occurred mainly between 12.3 and 13.6 Å. Calculations were then performed for C-like Mn XX and are shown overlapping the relative intensity trace in Figure 18. For the wavelength region of interest, there is good correspondence between theory and experiment, indicating that many lines in this spectral region belong to Mn XX transitions.

C. 12.643 Å region

A pair of TAP crystals were used in second order (2d spacing equal 12.877 Å) to record spectra centered at 12.643 Å corresponding to the F H beta line and spectra from Cr, Mn, and Ni in the high dispersion 2θ region equal to 158°. The red laser light was used to acquire spectra including the fluorine line from teflon targets while the green laser produced spectra from Cr and the two intense 2p-3s lines in Li-like Cr XXII which served as calibration lines. The reflectivity for second order TAP was found to be comparable to that of the beryl crystals. Therefore metal spectra could be acquired in single shots using red light while two shots with the green produced readable spectral patterns.

Spectrograms collected with the red laser light is shown in Figure 19 for the F, Mn, and Ni target emissions. The Doppler-shifted F H beta line occurs among a complex of Mn lines and in close alignment with a 2p-3d Ne-like Ni XIX line. The arrow in the spectrogram at 12.643 Å indicates a near coincidence between F H beta and an intense Mn line. Densitometer traces for the three spectra are shown in Figure 20. The F line is seen to align within a complex of overlapping Mn lines. Spectral identifications for Mn are largely unknown in this wavelength region. Atomic structure calculations have been performed for 2p-3d transitions in Be-like Mn XXII and B-like Mn XXI. The lines observed for Mn near 12.6 Å appear to belong to Be-like Mn XXII; however, the classification of lines will require detailed interpretation.

The spectrogram collected with the green laser light is shown in Figure 21 for Cr and Ni target emissions. The two intense 2s-3p lines in Li-like Cr XXII were used for wavelength determinations in the Ni spectrum. However, there is a considerable disagreement between the reported experimental and theoretical values for these two lines, as will be discussed in the next section. The Ni spectrum is a complex array of overlapping spectral lines as seen in the densitometer trace in Figure 22. This spectral region contains the 2p-3d transitions in Ne-like Ni XIX and their satellites in Na-like Ni XVIII. These satellite features have been identified in previous L-series spectra in Ti XII and Fe XVI[21]. The intense $2p^6$-$2p^5$3d (^{3}D) line in Ne-like Ni XIX may have a wavelength value near the wavelength for F H beta; however, experimental values have been reported ranging from 12.641 to 12.656 Å for this line. Atomic structure calculations were performed for 2p-3s transitions in O-like Ni XXI. Figure 23 shows the complex spectral region that exists for Ni from 12.4 to 12.9 Å. The spectral calibration shown in this figure is based on the theoretical values reported for Li-like Cr. An intense Ni line occurs at 12.651 Å that is an overlapping complex due primarily to the 2p-3d transi-

tion in Ni XIX and a 3d satellite for a $2p^6 3d - 2p^5 3d^2$ transitions in Na-like Ni XVIII. Lines that occur as shoulders on the central line have wavelength values of 12.646 and 12.661 Å. These shoulders possibly explain the experimental uncertainties in the previous measurements performed with less spectral resolution than that of the present work.

D. Survey Spectra

Three cylindrical-crystal spectrographs were used with convex-curved KAP crystals in order to collect the total K spectra from the teflon emission and L-series spectra from the transition metals. The survey spectrographs were used primarily as monitors of the X-ray spectral intensities. Spectral lines were recorded on Kodak No Screen film developed by standard techniques. Spectral data was acquired for multiple shots on each element. Before changing the shutter positions on the flat crystal spectrographs, the film in the survey spectrographs were developed to insure that sufficient X-ray emission had been accumulated to provide readable spectral lines. The KAP spectrographs recorded X-ray lines to 17 Å by using the ultra-thin stretched-polypropylene windows. This is evident upon examination of the fluorine spectra in Figure 24. The fluorine spectrum is generally similar to one obtained from previous laser work with a 1.05 um focussed beam.[22] The He alpha line has a wavelength value of 16.807 Å. This spectrum for the F K series lines was acquired in 2 shots of 200 psec pulses. Figure 25 shows the Ni L-spectrum acquired in a single, 200 psec shot with the red laser light. Transitions in Ne-like Ni are identifiable by pattern recognition such as the 2p-3s and 2p-3d, 4d lines shown in Figure 25. The regions covered by the high-dispersive flat crystal spectrographs are indicated in the figure. The need for high-resolution spectra to measure wavelengths of lines is evident.

IV. DISCUSSION

Many important factors have led to achieving wavelength values accurate to 1-3 mÅ in this work. These included the careful selection of experimental conditions and techniques, the use of limited-mass targets, the choice of and location of the two types of X-ray spectrographs, the availability of suitable X-ray spectrographs, the availability of suitable X-ray diffraction crystals, and the availability of precision densitometers for careful film measurements. Spectra were obtained with good resolution and dispersion to facilite high precision in determining wavelength values. Even with good spectrograms, the task of finding line coincidences to 0.1 eV is difficult in X-ray spectroscopy because of the spectral complexity and the difficulty of finding suitable lines with known wavelength values accurate to 1-2 mÅ to use as calibration standards. In addition, one must account for the line shapes due to Doppler motion. In selecting accurate calibration wavelengths, one finds difficulty for wavelength regions where suitable H- and He-like K-series lines are not available.

To achieve narrow X-ray line profiles requires a combination of a good crystal rocking curve and a small source size. Generally in collecting X-ray data from plasma emission, the finite source size dominates the

spectral line profiles. For the geometry used in this work where the source-crystal-film distance was 40-45 cm, the crystal broadening contribution corresponded to a source size of about 100-μm in diameter for the rocking curves of the beryl and TAP crystals. Two sets of targets were prepared having 75 and 450 μm diameters. Initial testing with the red light laser at 80J produced readable X-ray spectra in 1 to 3 laser shots depending on the relative line intensities for the lines of interest. This required the larger diameter targets. The smaller diameter targets were not tried because of concern as to shot-to-shot reproducibility for the large number of shots that would be required. Many test spectrograms were collected in the beginning of the study to determine that reproducibility could be achieved. It was found that reproducible spectral patterns could be achieved to the accuracy necessary, provided that the spectrographs remained stationary between shots and the targets were positioned to within 100 μm of the beam focus.

The X-ray line widths for the experiment were estimated from the dispersion relationship by accounting for the finite target size. With a 75 μm source, the line widths were estimated to be 2-3 mÅ and with 450 μm targets the estimated widths were 7-10 mÅ. The actual lines were found to have width of 9-12 mÅ using the beryl crystals for which the increase in width can be ascribed to Doppler broadening produced by the hot plasma. For the TAP crystals, the estimated lines would have widths 2.7 mÅ for 450 μm targets. The measured profiles were approximately 3 mÅ for the metallic targets. The fluorine lines were always broader and asymmetric due to Doppler motion shifts. The line widths recorded for the fluorine lines were found to be sensitive to the laser pulsewidth. Attempts to use laser pulses as long as 500 psec produced lines too broad to read. Little difference was noted between F lines obtained with shots of either 100 or 200 psec. The uncertainty in determining the Doppler shifts from the measured peak centroid was found to be about 1 mÅ. The X-ray lines recorded for the pair of diffraction crystals were broad being physically 0.4-0.6 mm in size because the finite plasma size was about 450 μm in diameter. The lines were read at low magnification with a long slit on the comparator densitometer. The center of the slit was placed between the two spectral strips and both halves of the Decker slit system were aligned to match the line profile and tilt. This compensated for the slight curvature in the lines due to the Kossel effect. It was determined that the centroids of the lines could be measured to a few tens of microns such that precisions of 1 mÅ or less were obtainable.

Once the line positions were precisely known, the accuracy in the wavelength determination was dependent on knowing accurate calibration lines. The L-and M-series X-ray wavelengths from higher atomic elements have been based on wavelengths of K-series lines, generally the H-and He-like lines. The wavelengths of K-series transitions have been calculated to a high degree of accuracy. When possible one tries to use K lines for wavelength calibrations. In this work at high spectral resolution, the number of choices is limited for the narrow spectral regions that were recorded. Therefore suitable known wavelengths in the L-series were

needed. The Ne-like lines in L-series spectra are generally distinct and well measured. However, the spectral ranges covered in each spectrogram are less than one Angstrom. The only Ne-like lines that occurred in the regions of interest were those of Ni XIX for which a wavelength disagreement exists for published values. Another isoelectronic sequence that has been carefully studied has been the F-like ions. Fortunately many strong 2p-3d transitions in Fe XVIII exist in the 14.0-14.6 Å region and can be used to calibrate the data collected with beryl at 129°. In the 13.3-14.0 Å region that was recorded with the beryl crystal set at 120°, only a few weak lines from F-like Co XIX occur in this region; therefore, suitable F-like calibration lines are not available near 13.781 Å. For the latter region the choices for calibration lines were to use the Doppler-shifted F lines in the red light experiment or the Be-like Cr lines in the green light study.

The F-like Fe XVIII spectral patterns were read a number of times from spectrograms collected in the two experiments at the two different angles. The calibration for the intense lines agreed within the 1-2 mÅ uncertainty found in the published values, and the weaker lines near 14.458 Å were measured with a wavelength accuracy of ∿3 mÅ. It was found that the Doppler-shifted F lines could be determined to a high precision. For the spectrograph positioned at ϕ=126° the Doppler shifts were between +3.5 and +5 mÅ and they were between +6 and +8 mÅ for the spectrograph that looked toward the ion velocity distribution at ϕ=180°. This established an ion velocity in fluorine relative to the Fe ions of 1-2 X10^7 cm/sec. The same values for the Doppler shifts were applied to the F He gamma line in the 120° data. The measured wavelengths were in agreement for the two sets of calibrations.

The most troublesome region to calibrate was the 12.4-12.8 Å spectral region collected with the TAP crystal. A value for a 2p-3d Ne-like Ni transition was reported at 12.641 Å[23] that is nearly coincident with F H beta line at 12.643 Å. However, more recent values for the 2p-3d line in Ni are 12.654 Å,[24] 12.656 Å[5] and 12.657 [25]. These agree more closely with a theoretical value predicted to be 12.653 Å. Fortunately, another alternative for calibrating this region existed using the intense 2p-3s line in Li-like Cr. However, the work by Aglitskii[10] points out a large uncertainty of 7 mÅ existing between the theoretical studies and the experimental values for Li-like Cr. The two independent experiment studies report higher values for the Cr lines. In this work the wavelengths determined for using the Doppler-shifted F lines agreed within 3 mÅ to the values determined using the experimental wavelengths for Li-like Cr.

Examination of the wavelength values in Table 1 indicates a number of wavelength coincidences exist between the K and L spectra based on wavelength matching. Another part of the selection of line coincidences is the knowledge of the X-ray line intensities. This requires absolute calibration of diffracting crystals and film sensitivities. The SB-5 film has been studied and one set of values exist corresponding in wavelength to Cu L α radiation, which were used in this work. The relative intensities obtained in the spectral traces in this work are based on theoretical R-values determined for other beryl crystals. The R-values for the speci-

fic beryl and TAP crystals used in this work remain to be measured so that absolute line intensities can be determined. However, another step in determining absolute line intensities is the need to classify the complex spectral lines. The identifications given in this report are tentative and based solely on alignment with atomic structure calculations. A more definitive classification of lines will require a thorough spectroscopic analysis. This will involve working out selected energy level diagrams and interpolation from isoelectronic sequences.

Further improvements or refinements in the data might possibly be made by reducing the plasma source emission per shot. With the present experimental conditions, this would require a pile-up of many laser shots which can be achieved but would be expensive. Another approach would be to generate plasma sources of a few tens of microns diameters using an implosion geometry. Metallic-coated or doped-glass microballoons filled with the appropriate lasant gas could provide adjacent pump and lasant spectral lines by using spatially-resolving techniques.

V. CONCLUSIONS

The goal to measure X-ray wavelengths in L-series spectra from transition metals to within 1-3 mÅ was achieved.

A number of L-series pumping candidates were found that had lines nearly coincident with He- or H-like fluorine lines. The 12.641 Å line in Mn XXII is near the value of 12.643 Å for the F H beta line. Possible line coincidences occur in Cr XXI and Ni XX that match the weak F He delta line within 4 mÅ. In the vicinity of the F He beta line at 14.458 Å are line coincidences occurring in Cr XX and Mn XIX. These lines coincide with the He beta line to within 1-2 mÅ. No candidate line was found that matched the F He gamma line.

In a lasing experiment, one might choose Mn as a pumping candidate because of the lines at 14.458 Å and at 12.641 Å which are in near coincidence with the intense F He beta and F H beta lines.

ACKNOWLEDGEMENTS

This work was supported by the I.C.F. Program under the Division of Laser Fusion of the U.S. Department of Energy and funded through the Novette Laser program at Lawrence Livermore National Laboratories. We wish to acknowledge Peter Hagelstein and Art Toor for suggesting the basic need for conducting this study and the valuable discussions with Dennis Matthews at LLNL. The authors are in debt to the entire crew at KMS Fusion for their support and fortitude in making this a successful effort, in particular Don Slater, Roy Johnson and Eric Storm. Appreciation goes to David Steinman for his persistence in target fabrication and to Robert Schroeder and David Sullivan for assistance in the collection of the X-ray data. One of us (P.G.B.) wishes to express gratitude to Barry Kent of the Space and Astrophysics Division at the Rutherford Laboratories for the loan of the valuable beryl crystals that made the experiment possible. Special thanks go to Brian Sweeney of Sachs/Freeman Associates for his diligence in the computer processing of the data.

Table 1

Lasant	λ(Å)	Pump Line	λ(Å)red	λ(Å)gn	Transition
F He_β	14.458	Fe XVIII* (F-like)	14.453[a]	14.453[a]	2p-3d
			14.469[a]	14.469[a]	2p-3d
		Cr XX (B-like)	14.458	14.457	2p-3d
		Mn XIX (N-like)		14.458-14.459	2p-3d
F He_γ	13.781	Cr XXI* (Be-like)	13.774	13.775[b]	2p-3d
		Fe XIX (O-like)		13.767	2p-3s
		Mn XX (C-like)		13.794	2p-3d
		Ni XIX (Ne-like)	13.788		2p-3s
F He_δ	13.488	Cr XXI (Be-like)	13.493	13.492	2p-3d
		Ni XX (F-like)	13.491		2p-3s
F H_β	12.643	Ni XIX (Ne-like)	12.655	12.657[c]	2p-3d
				12.651[d]	
		Mn XXII (Be-like)	12.641		2p-3d
		Cr XXII* (Li-like)		12.662[c]	2p-3s
				12.656[d]	2p-3s
				12.664[e]	2p-3s

* Transitions used for calibration.

a) Fe XVIII wavelength values from H. Gordon, et al (1980).

b) An average value for Cr XXI from work of N. Spector, et al (1980) and V.A. Boiko, et al (1978).

c) Based on the experimental values for Li-like Cr XXII transition reported by S. Goldsmith, et al (1972).

d) Based on the theoretical value for Cr XXII from B. Edlen (1979).

e) Experimental value for Cr XXII from E. V. Aglitskii, et al (1975).

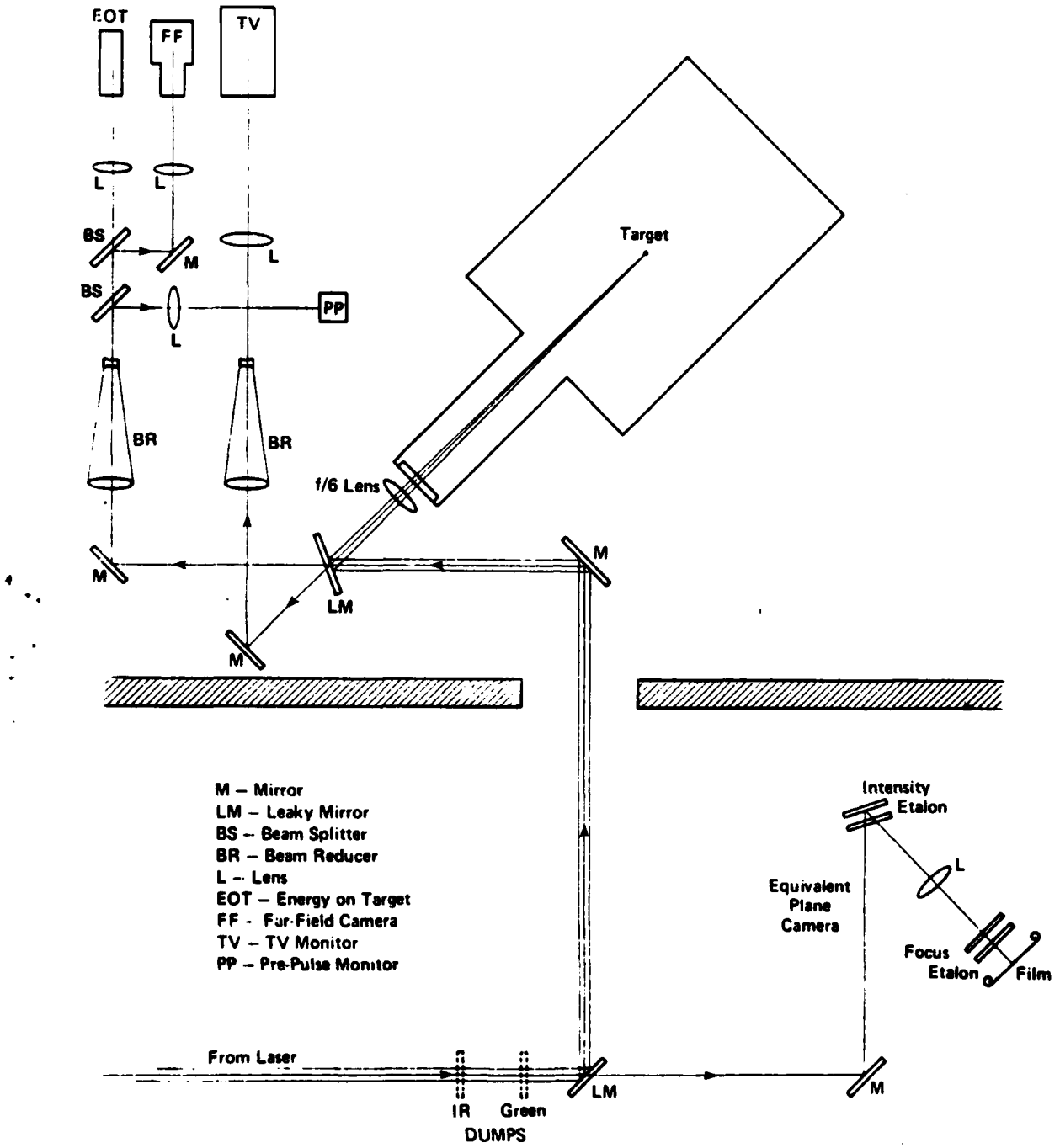

Figure 1. Schematic of laser diagnostics.

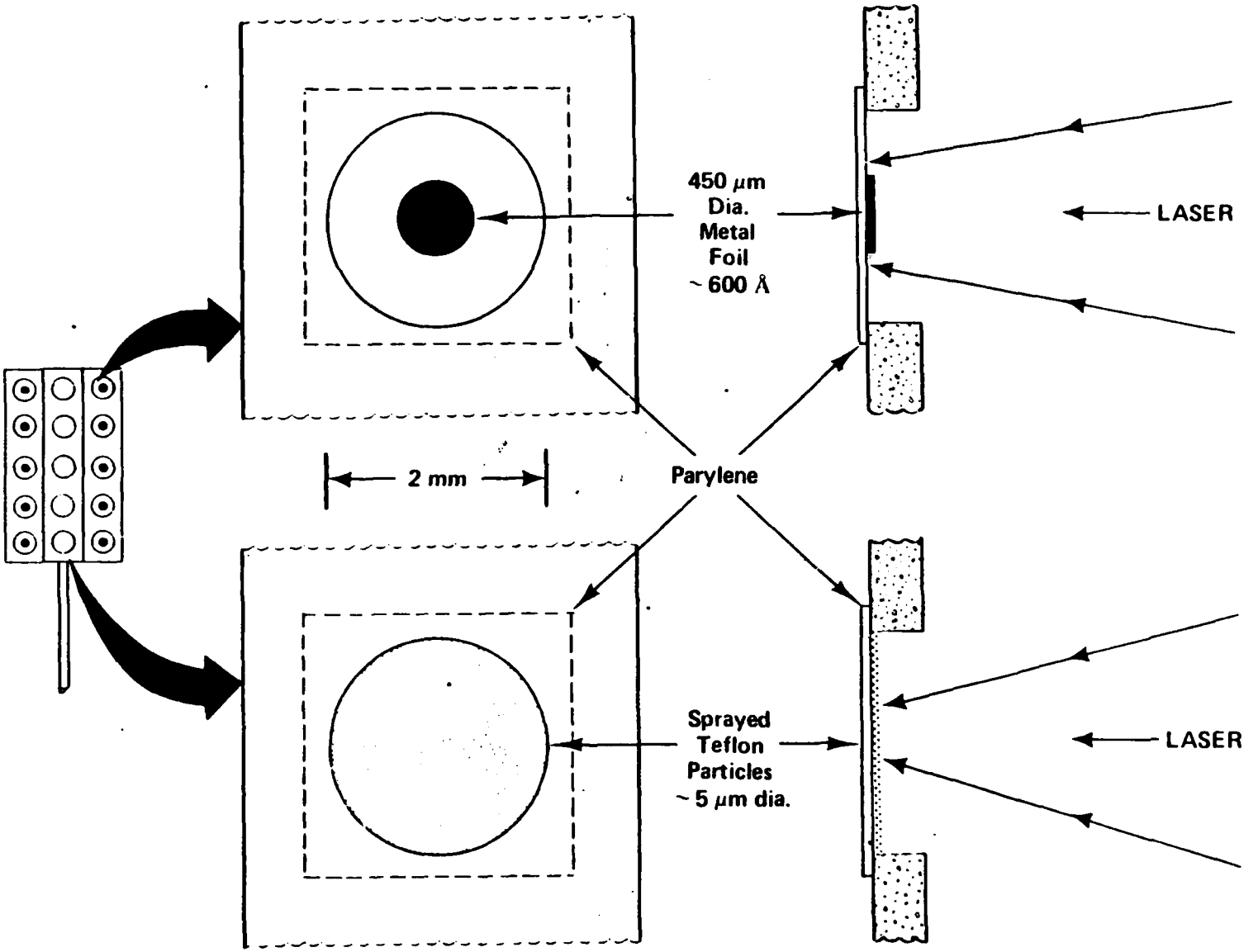

Figure 2. Schematic of target types and irradiation.

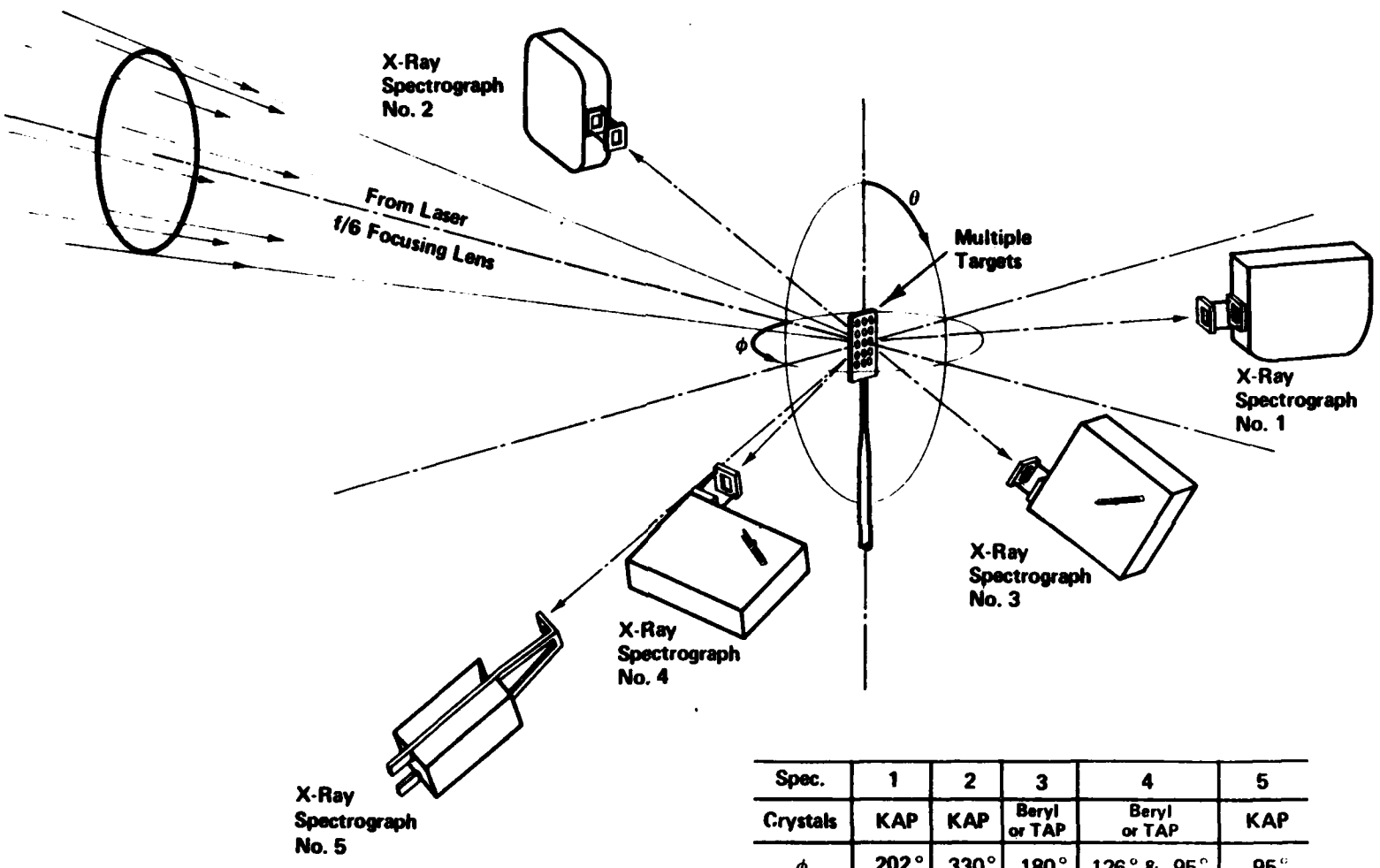

SCHEMATIC ARRANGEMENT OF THE CRYSTAL SPECTROGRAPHS

Spec.	1	2	3	4	5
Crystals	KAP	KAP	Beryl or TAP	Beryl or TAP	KAP
ϕ	202°	330°	180°	126° & 95°	95°
θ	90°	90°	125°	90° & 120°	135°
Distance to Film	30.1	30.1	45	44	30 cm

ϕ Measured from laser axis, in horizontal plane

θ Measured from vertical axis through target

Figure 3. Schematic of X-ray crystal spectrograph geometry.

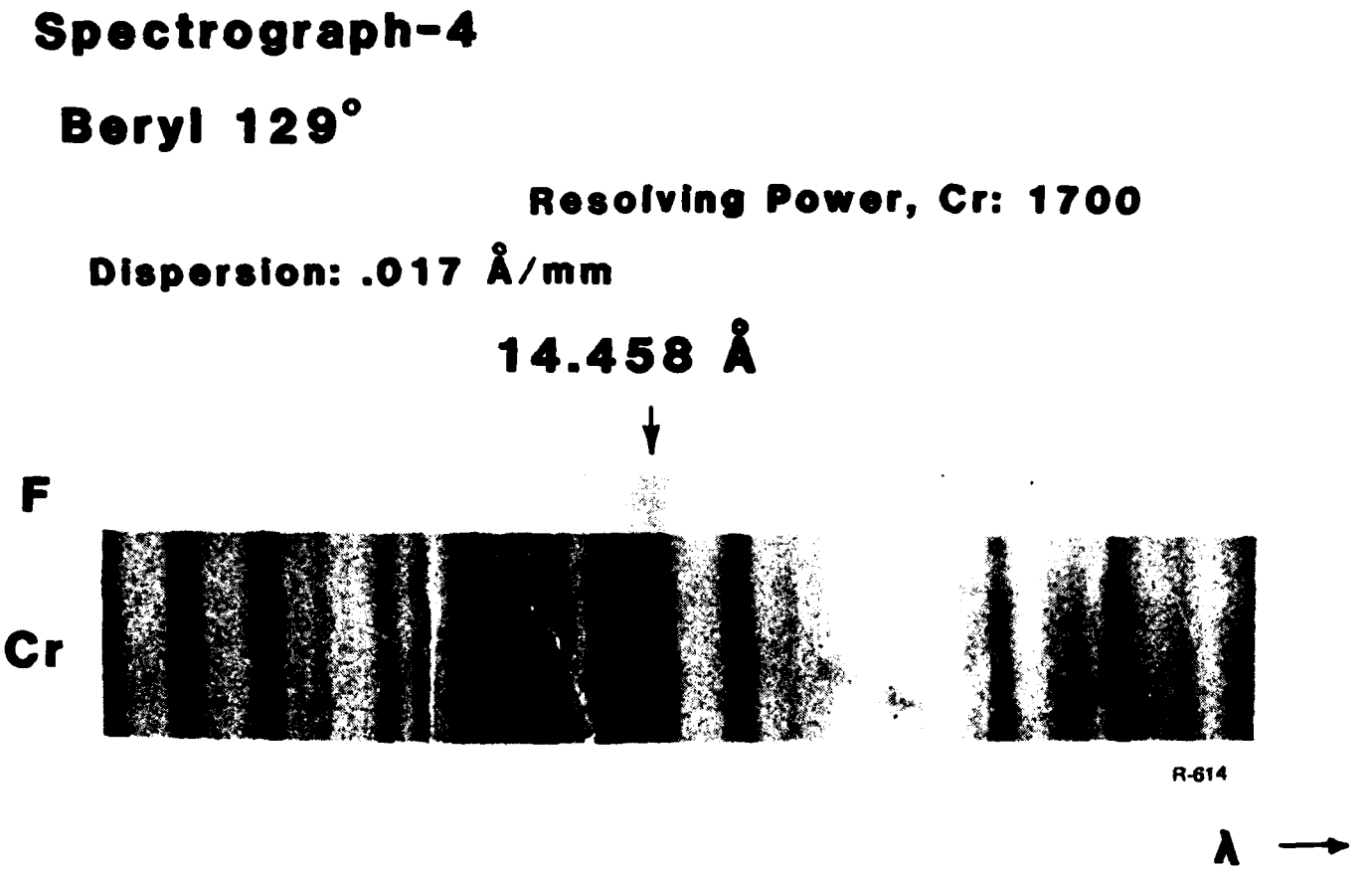

Figure 4. Spectrogram recorded from F and Cr emissions with the beryl crystal spectrograph at a Bragg angle ($2\theta=129^{\circ}$). The spectra were acquired with the red laser light with 2 shots of 200 psec each for Cr and 3 shots of 100 psec duration for the teflon target.

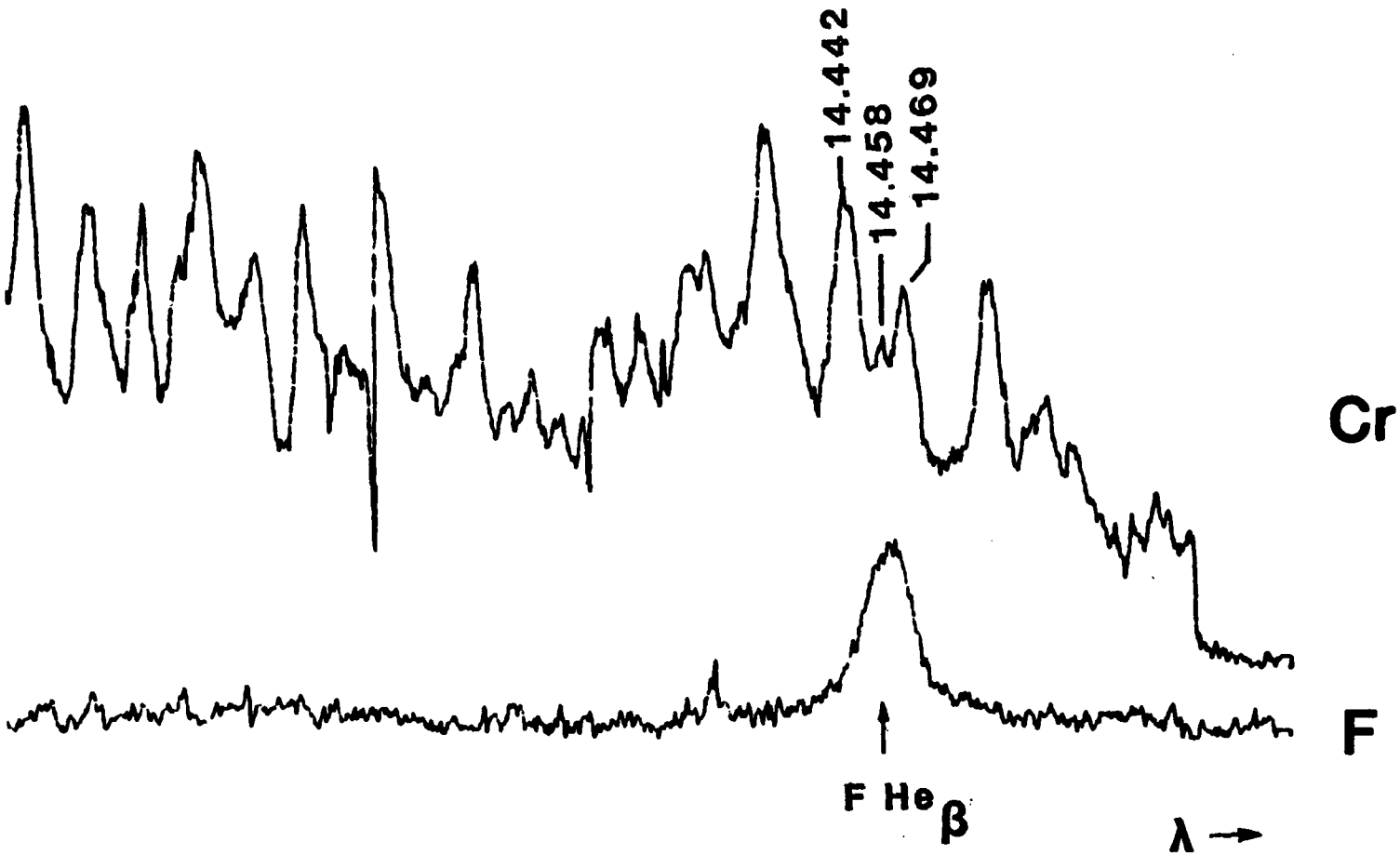

Figure 5. Densitometer traces of F and Cr spectra collected with red light.

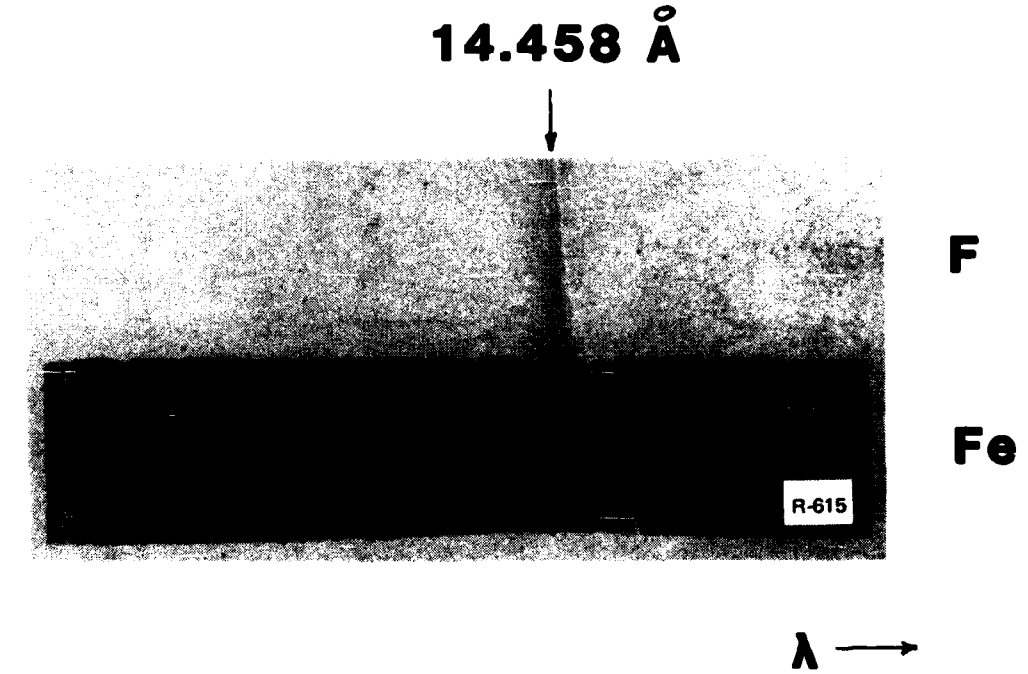

Figure 6. Spectrogram collected from F and Fe emissions with the beryl crystal spectrograph at 129°. Both spectra were acquired in three shots of 100 psec duration using red light.

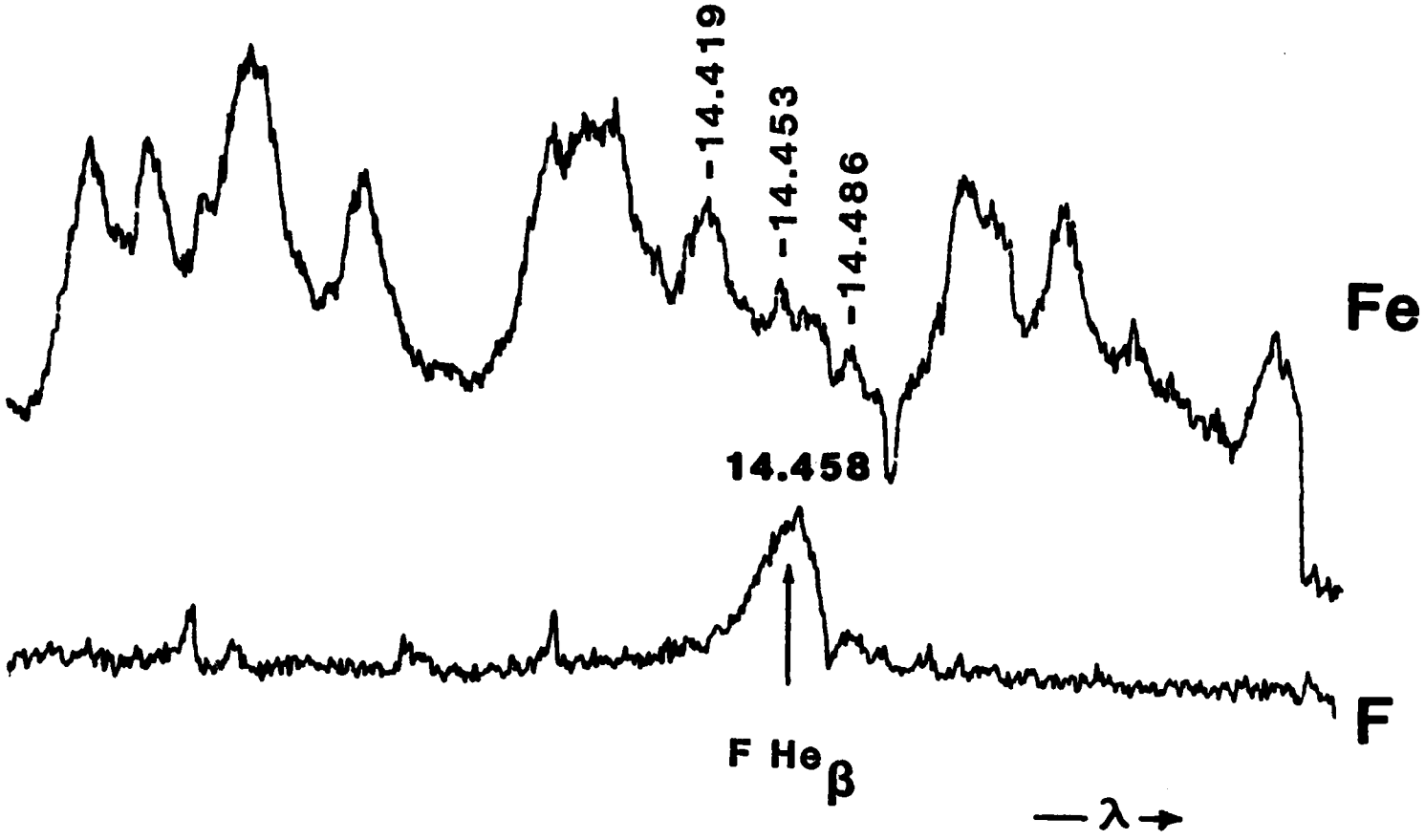

Figure 7. Densitometer traces of F and Fe spectra collected on the spectrogram shown in Fig. 6.

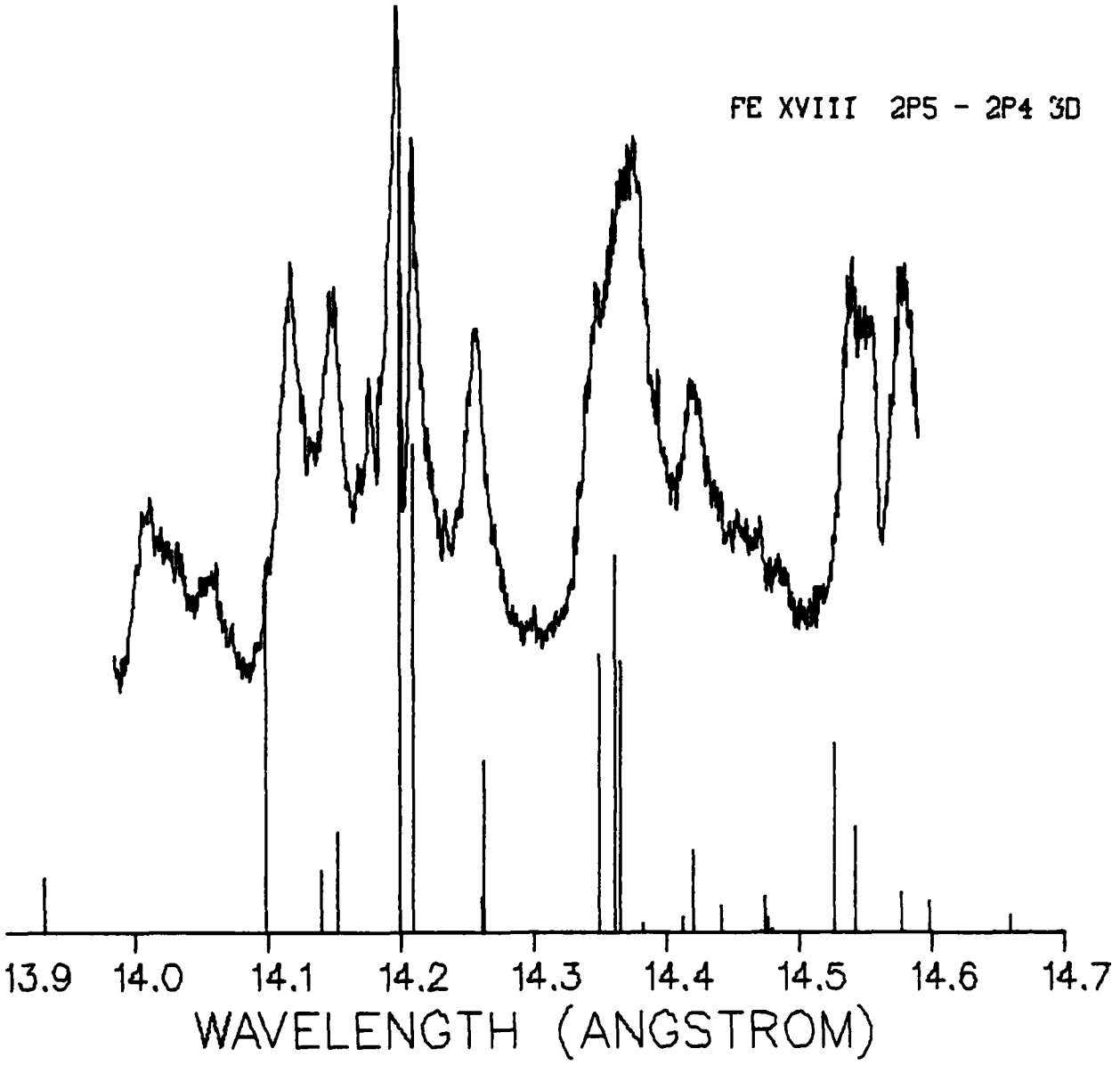

Figure 8. Intensity spectrum of Fe in the 14.0-14.6 Å region together with atomic structure calculations for the 2p-3d transitions in F-like Fe XVIII. The theoretical lines have their heights plotted proportional the theoretical oscillator strengths, (gf-values).

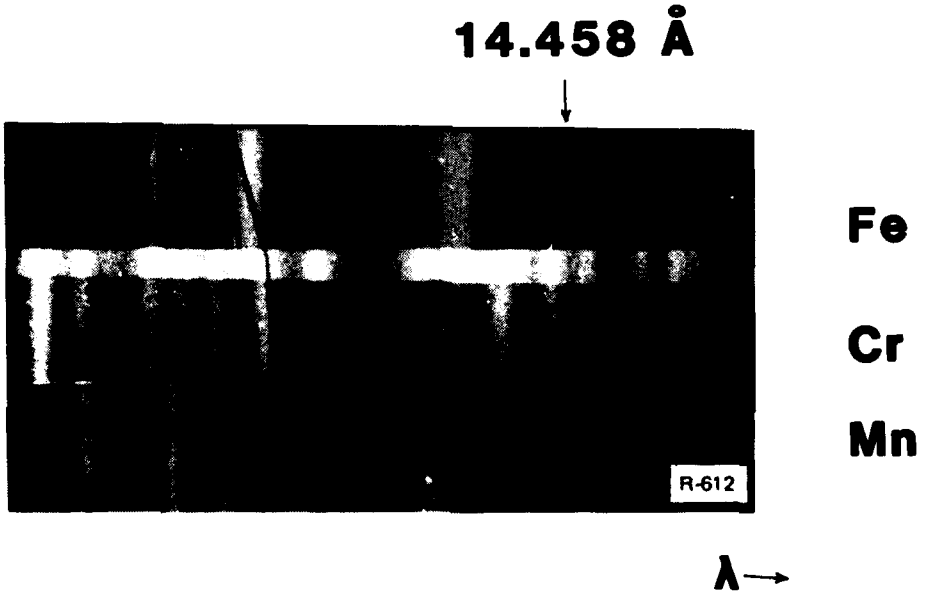

Figure 9. Spectrogram recorded from Cr, Fe, and Mn emission with the beryl crystal at 129°. The spectra were recorded in two shots each of 100 psec duration with the green light laser.

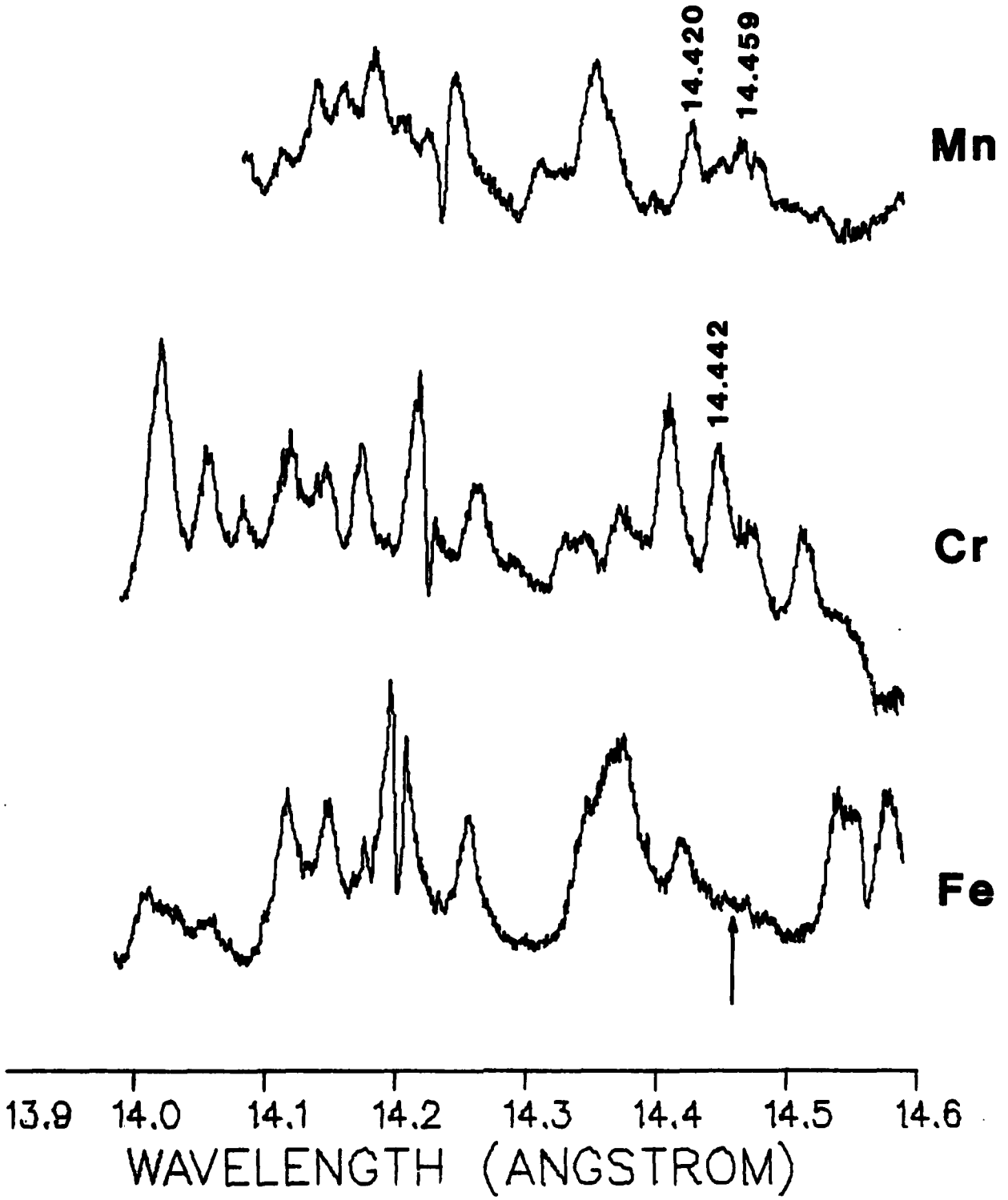

Figure 10. Spectra of Cr, Mn, and Fe in the wavelength region of 14.0-14.6 Å.

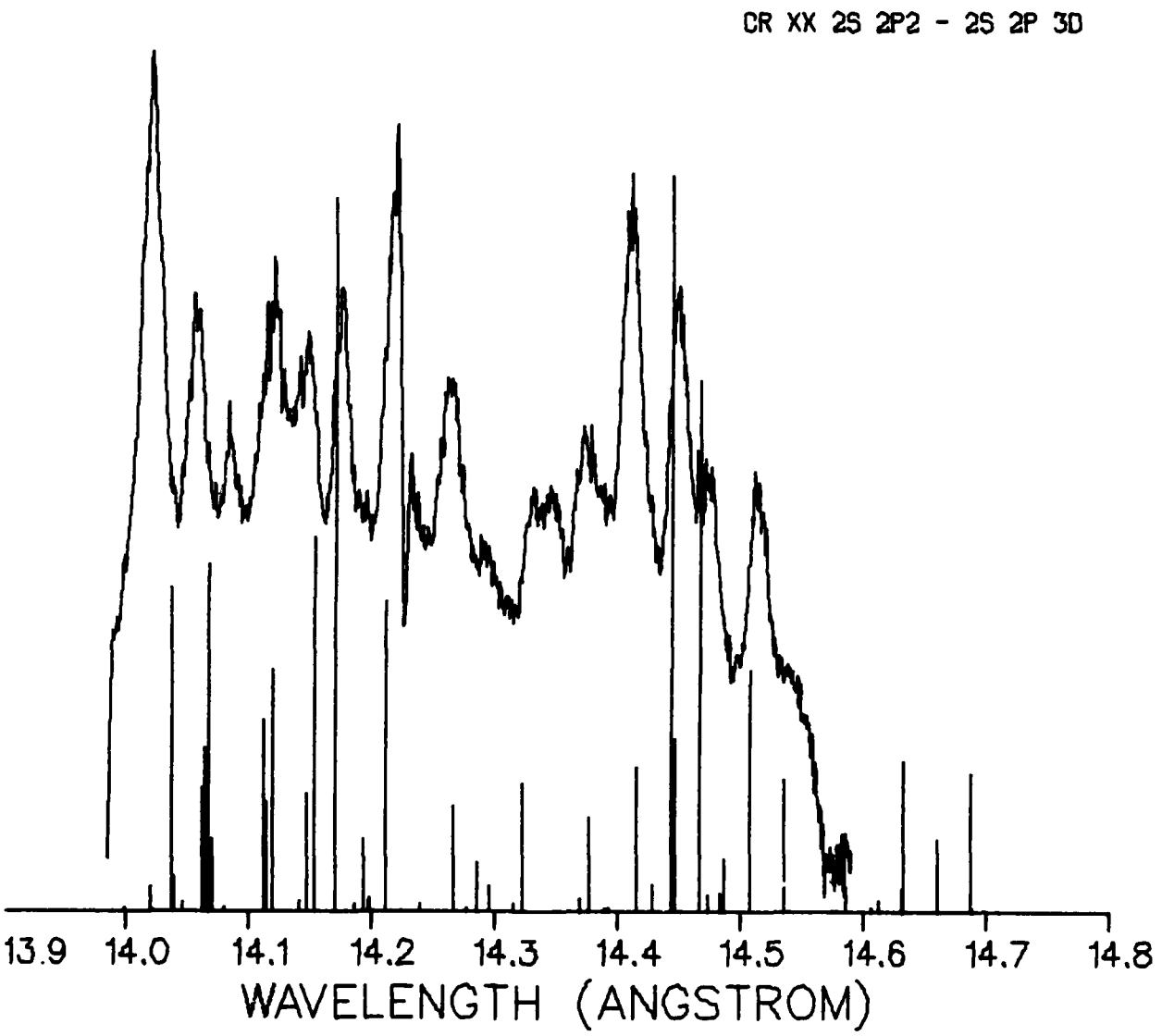

Figure 11. Cr spectrum together with atomic structure calculations for B-like Cr XX.

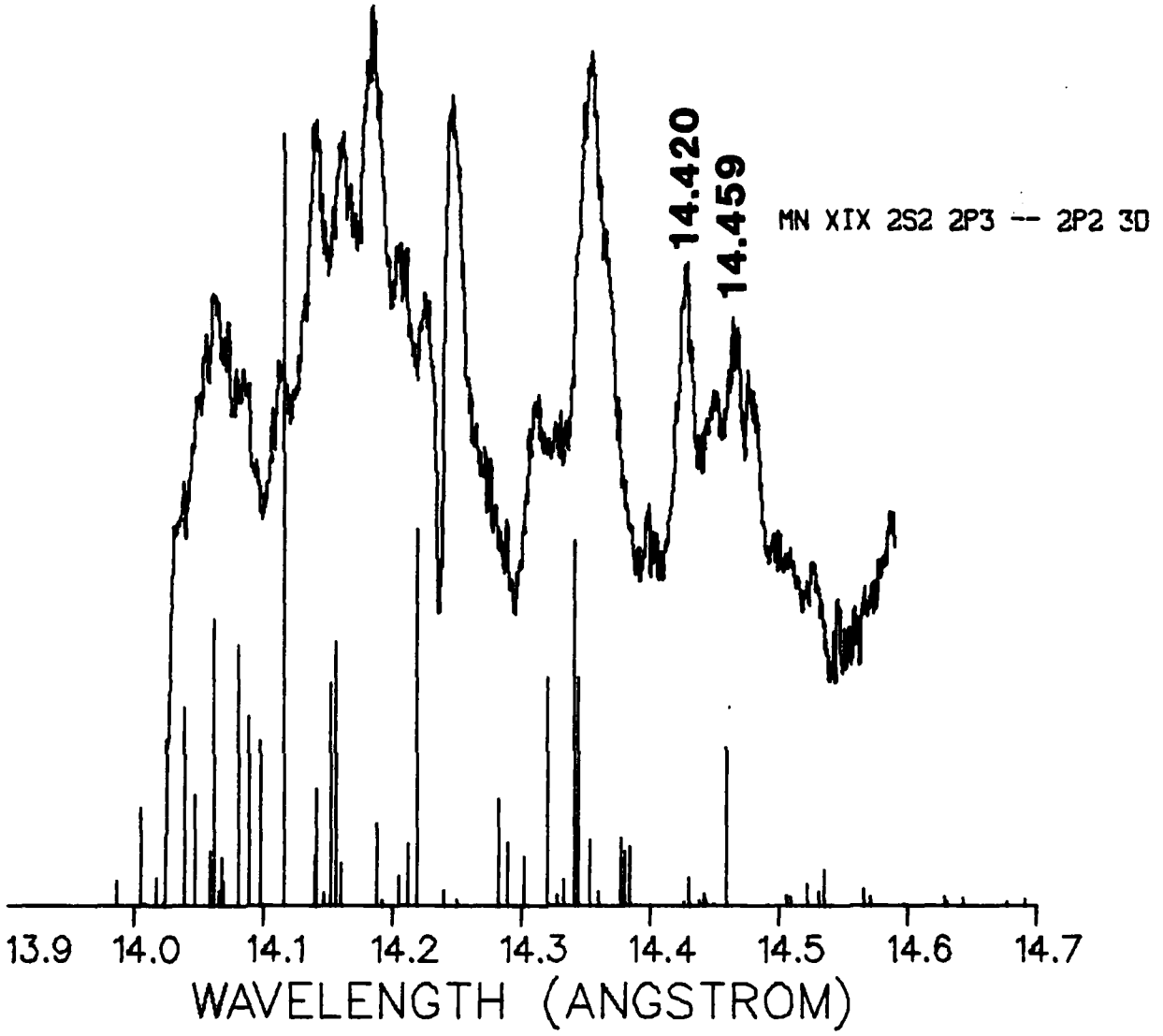

Figure 12. Mn spectrum together with at. structure calculations for N-like Mn XIX.

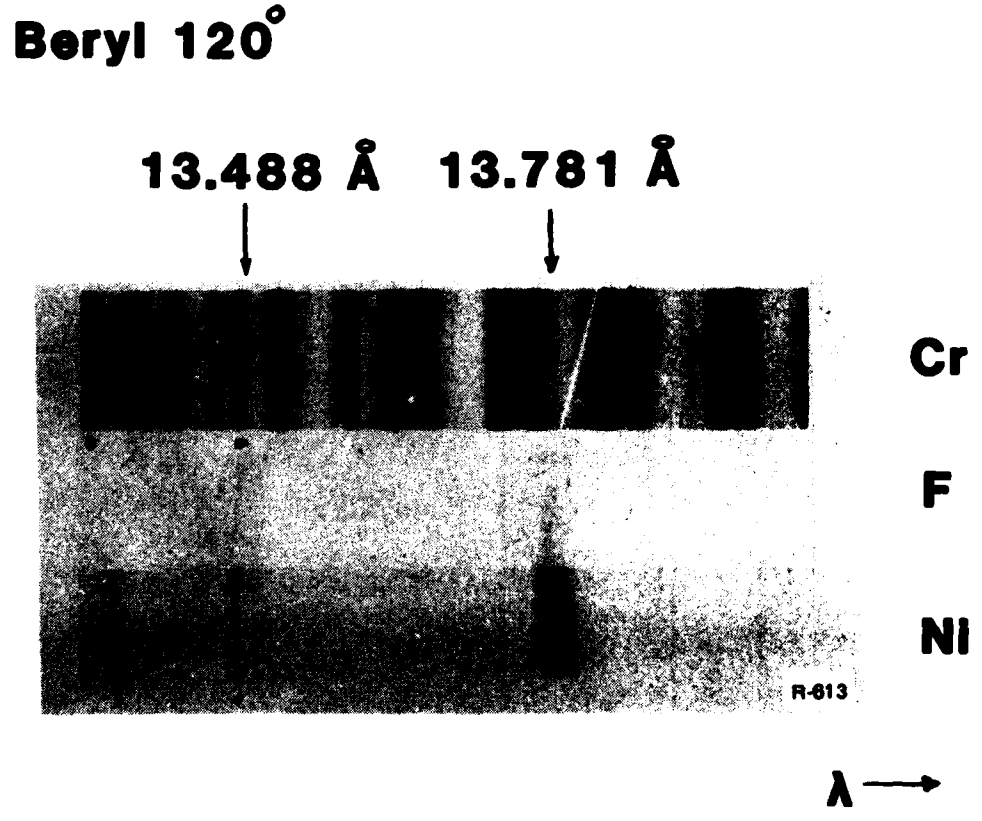

Figure 13. Spectrogram recorded from F, Cr, Ni emission with the beryl crystal at 120°. The fluorine spectrum required three shots while the metals were recorded with one shot all at 200 psec of red light.

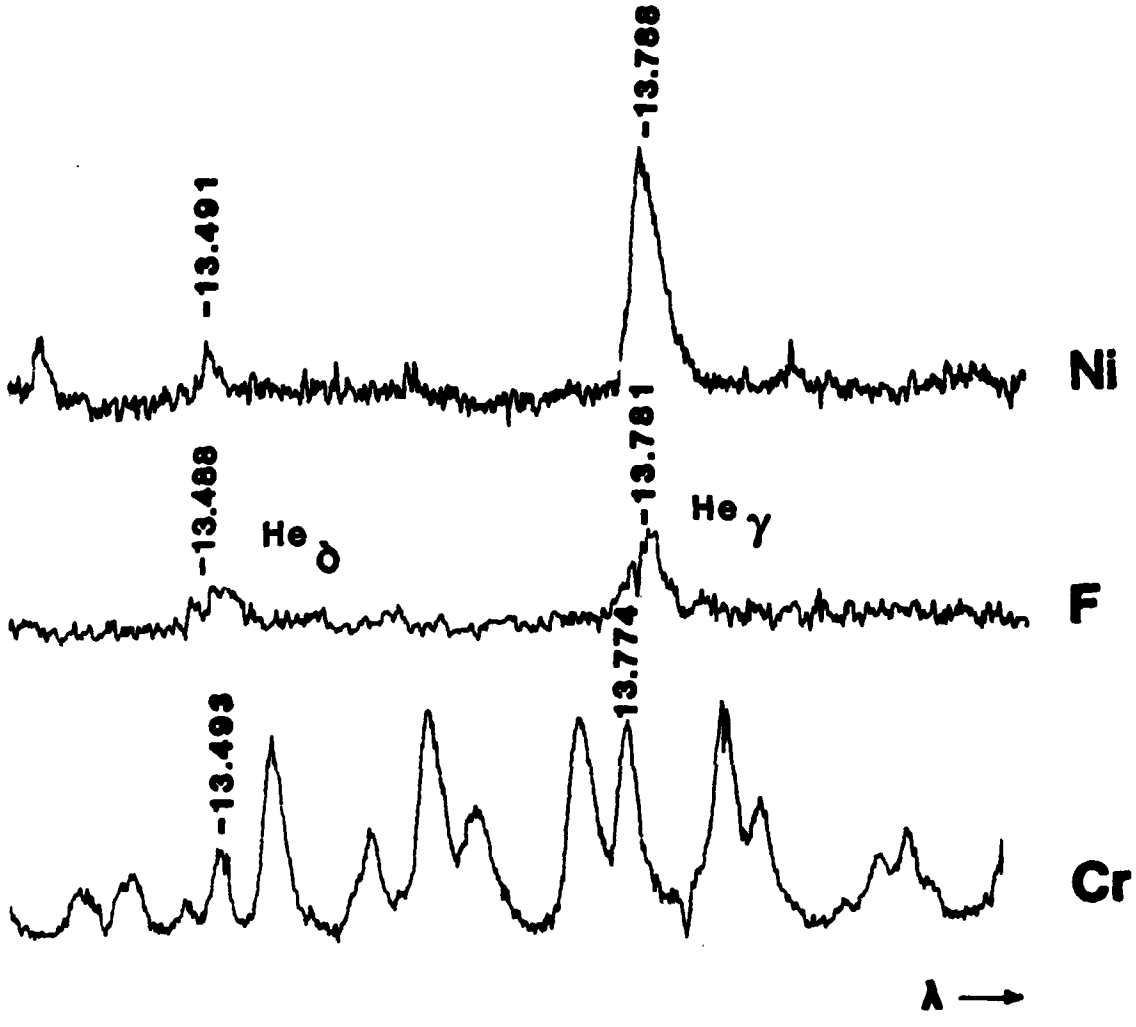

Figure 14. Densitometer traces of F, Cr, and Ni from the spectrogram shown in Fig. 13. Line coincidences can be seen with both the F He gamma and He delta lines.

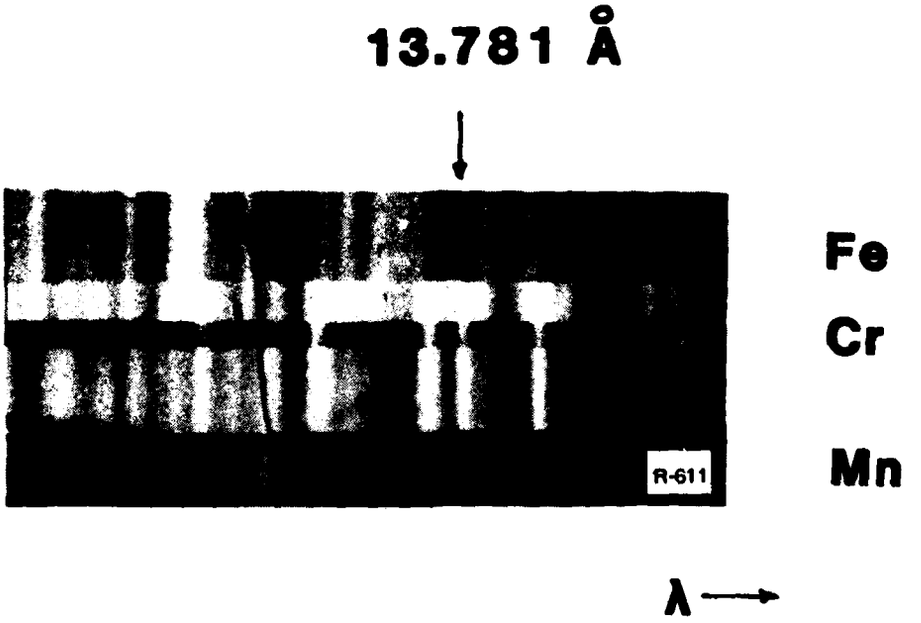

Figure 15. Spectrogram recorded from Cr, Fe, and Mn emission with the beryl crystal at 120°. The spectra were recorded with two shots each of 100 psec duration of green light.

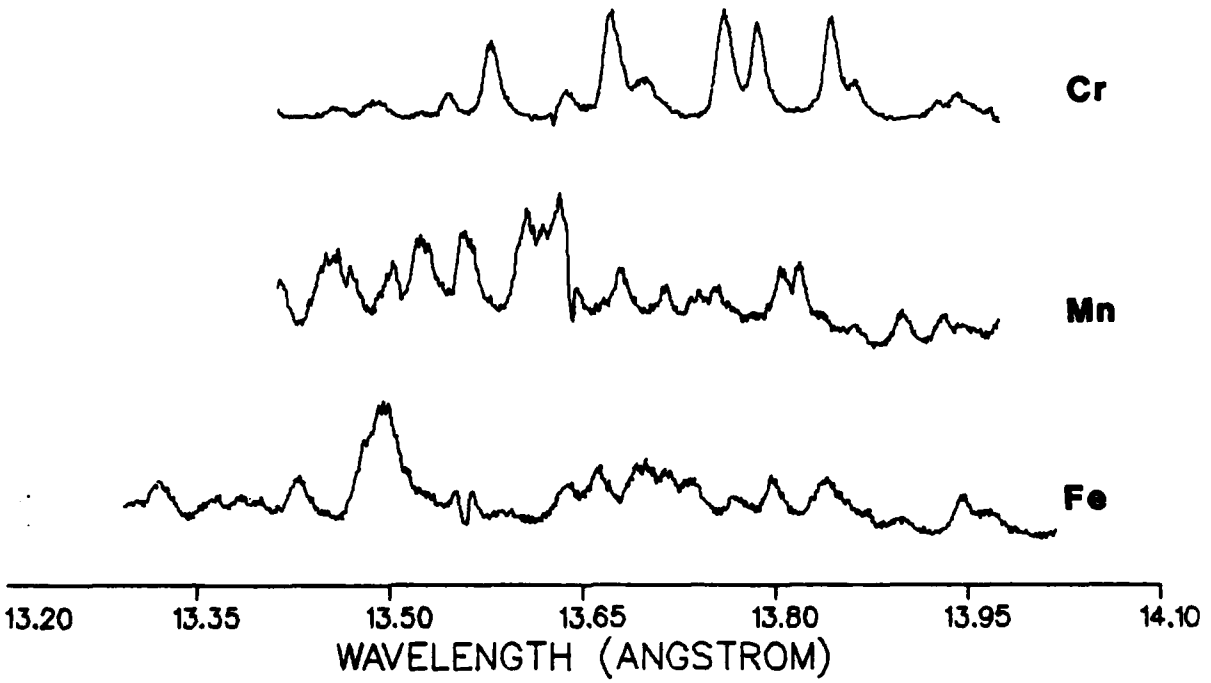

Figure 16. Spectra of Cr, Fe, and Mn from the 13.3-14.0 Å region from the spectrogram in Fig. 15.

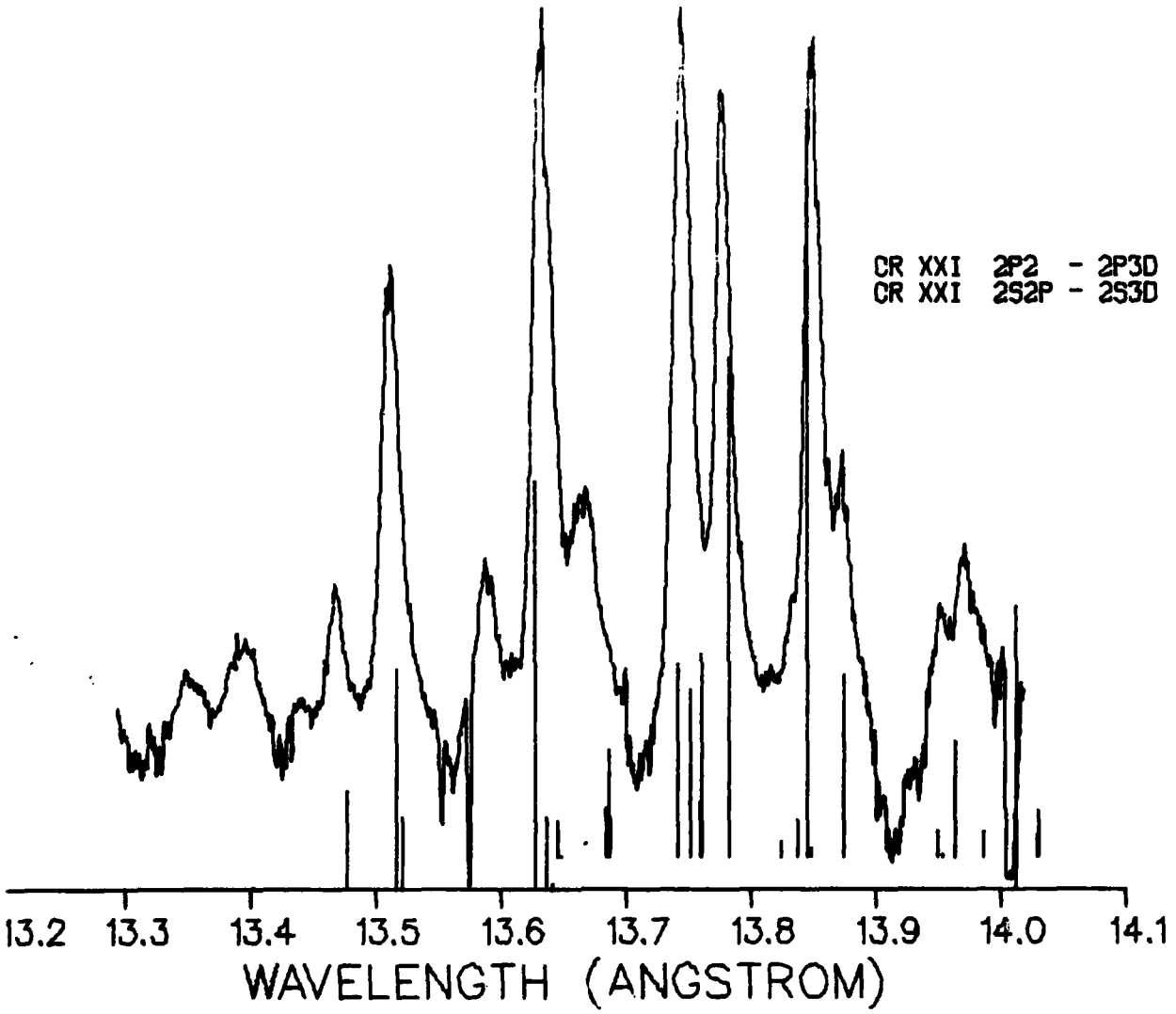

Figure 17. Cr spectrum and at. structure calculations for Be-like Cr XXI.

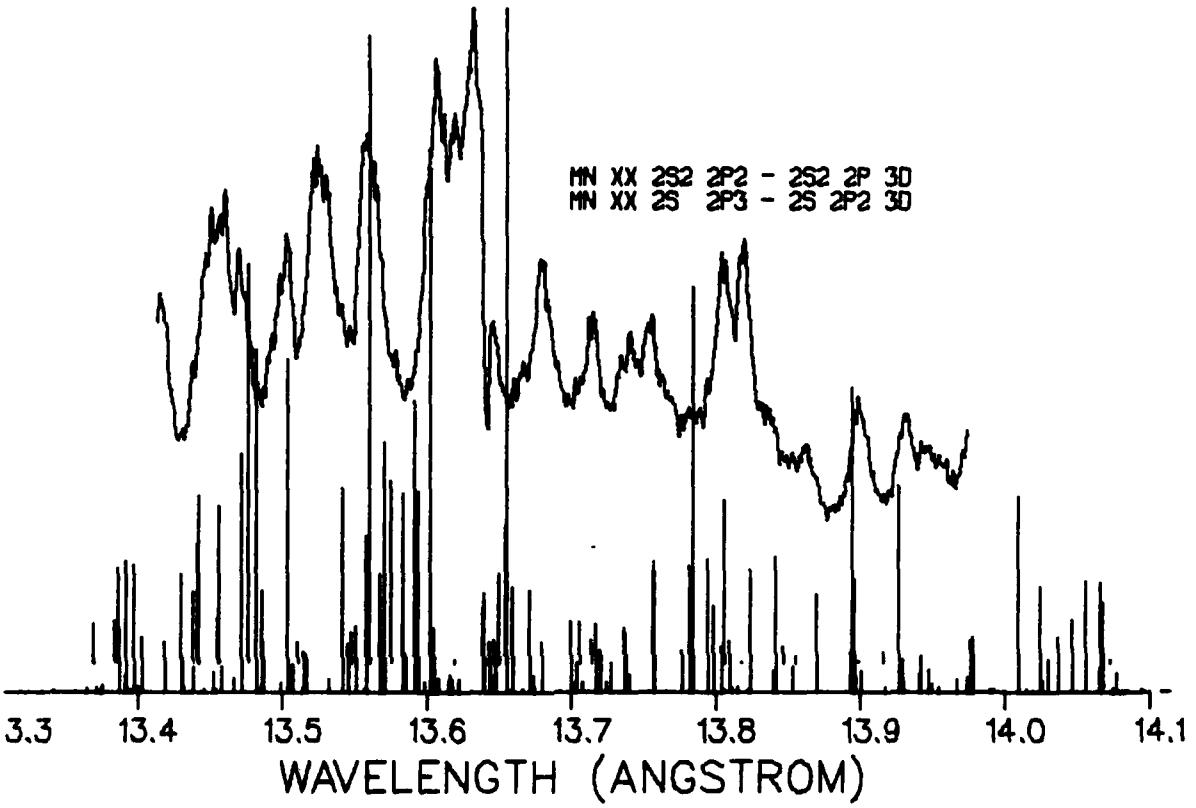

Figure 18. Mn spectrum and at. structure calculations for C-like Mn XX.

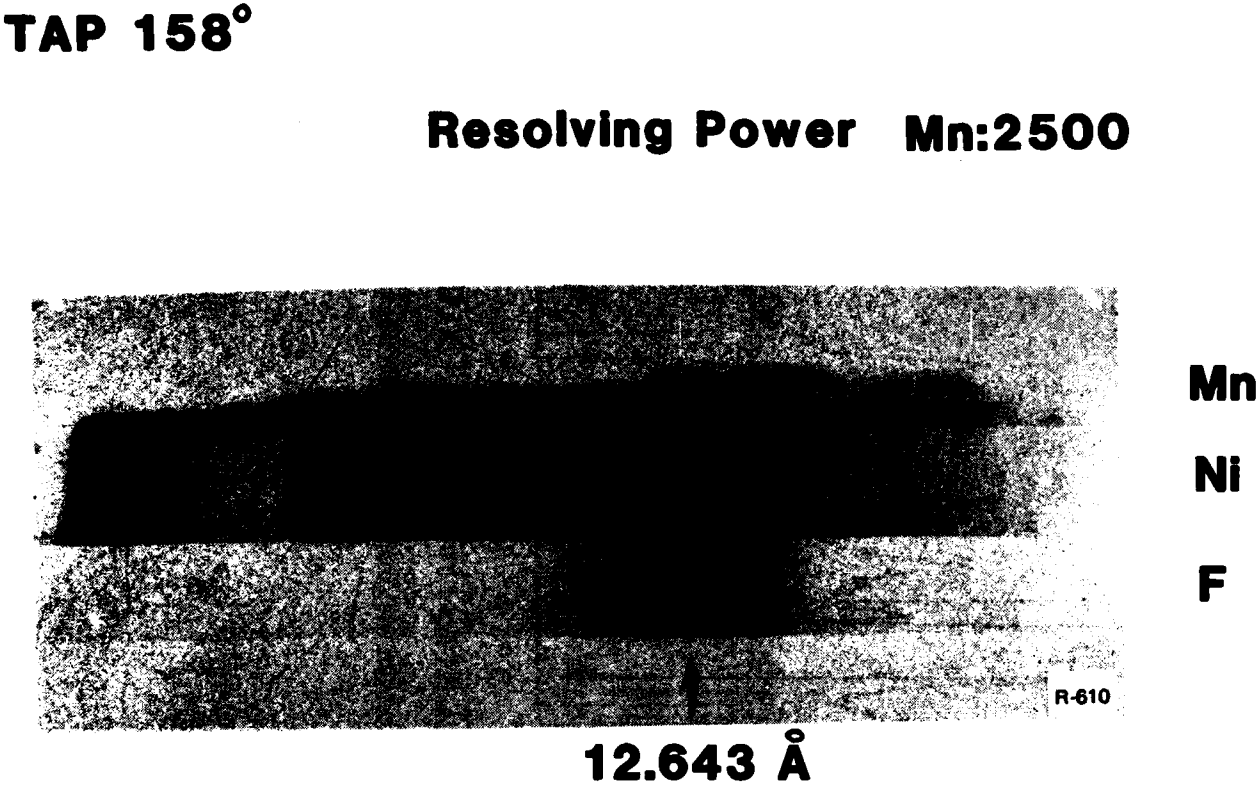

Figure 19. Spectrogram of F, Mn, and Ni collected with the TAP crystal at 158°. The Mn and Ni spectra required one shot each of 200 psec while the F spectral line was collected in 3 shots of 100 psec using red light.

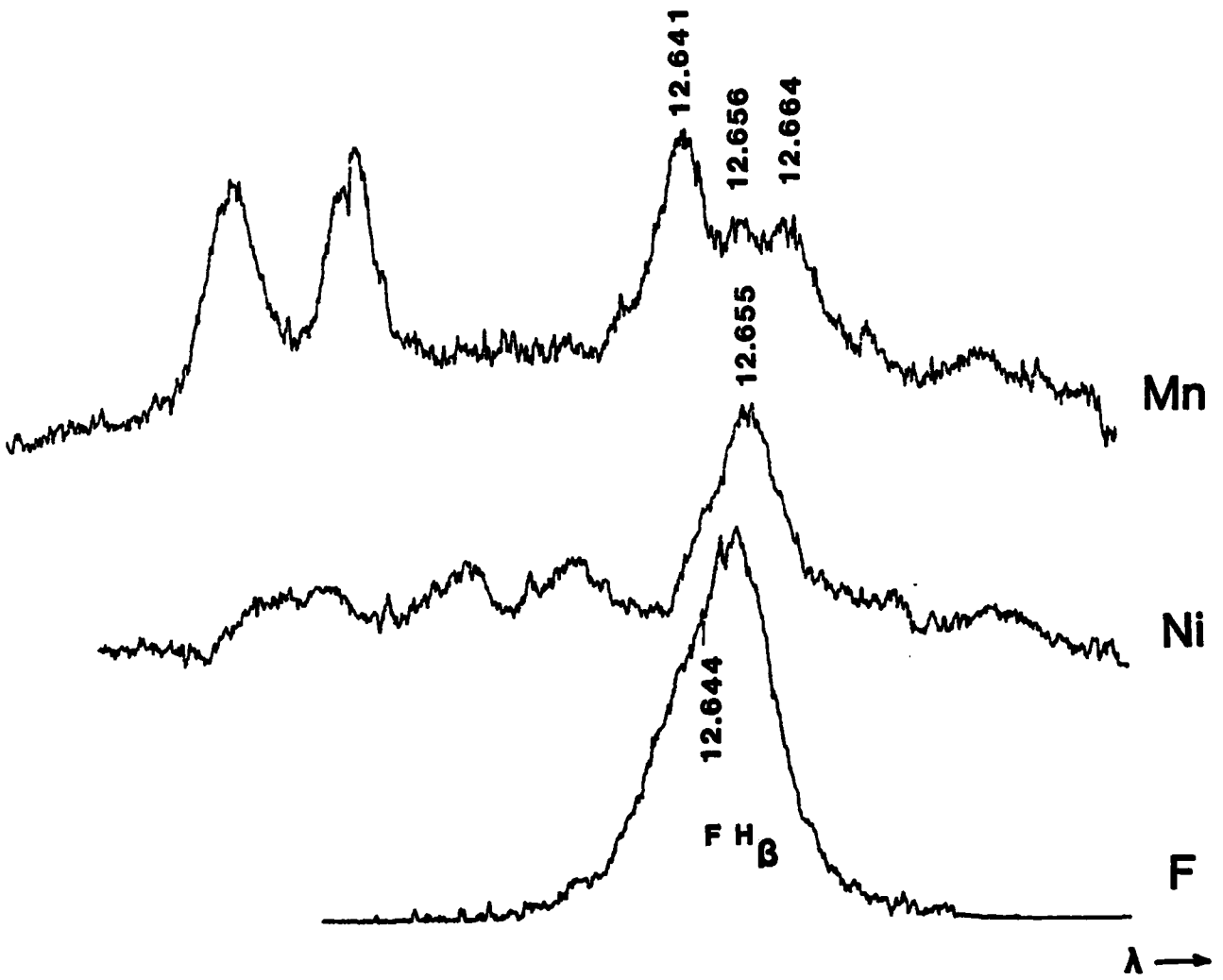

Figure 20. Densitometer traces of the spectrogram shown in Fig. 19.

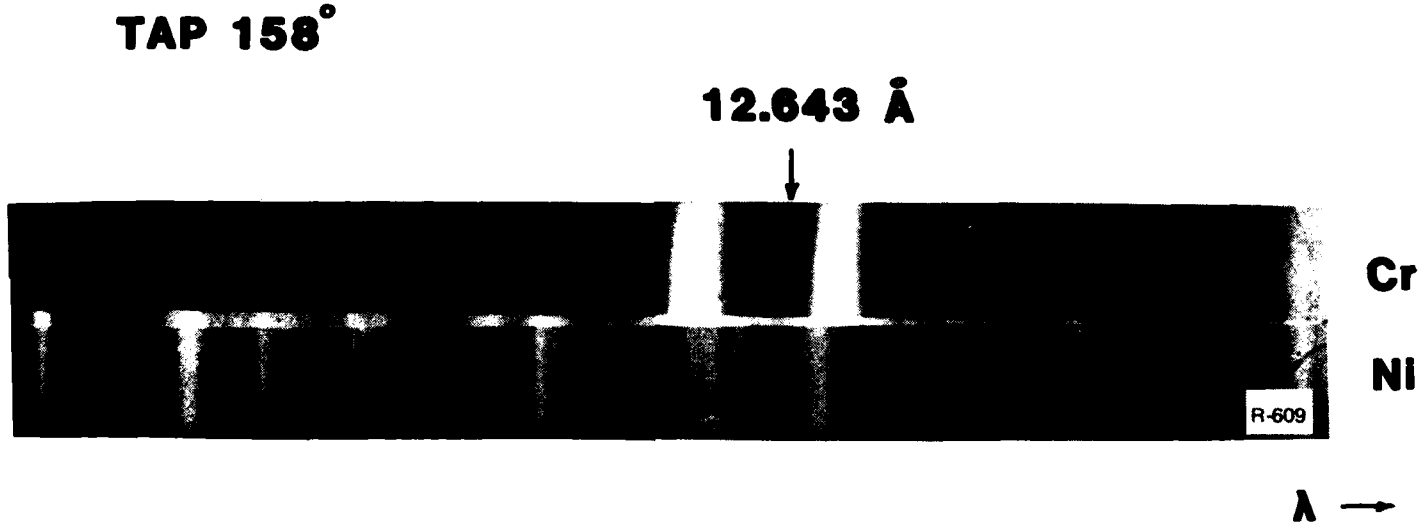

Figure 21. Spectrogram of Cr and Ni collected with the TAP crystal with green light.

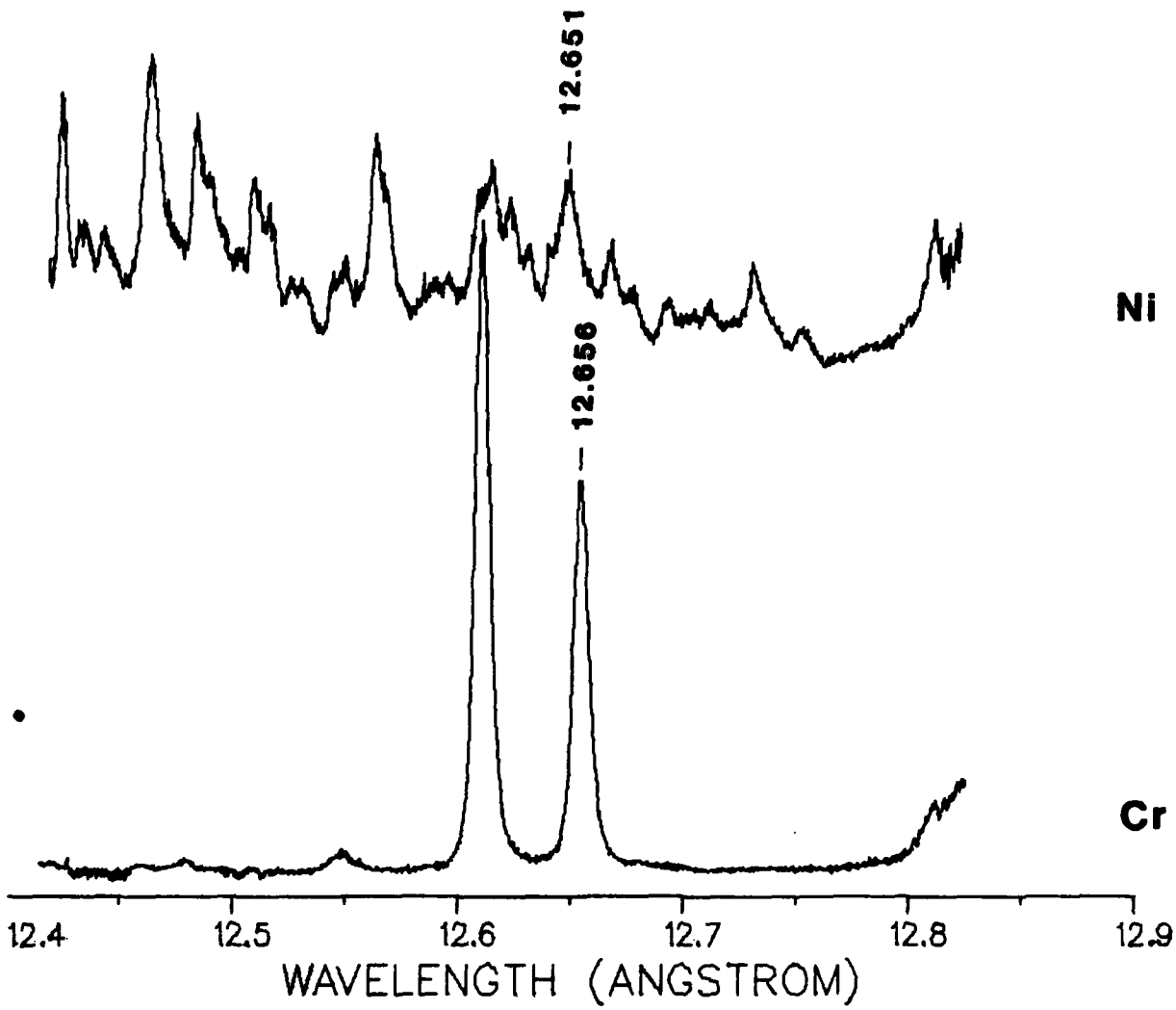

Figure 22. Spectra of Cr and Ni for spectrogram shown in Fig. 21.

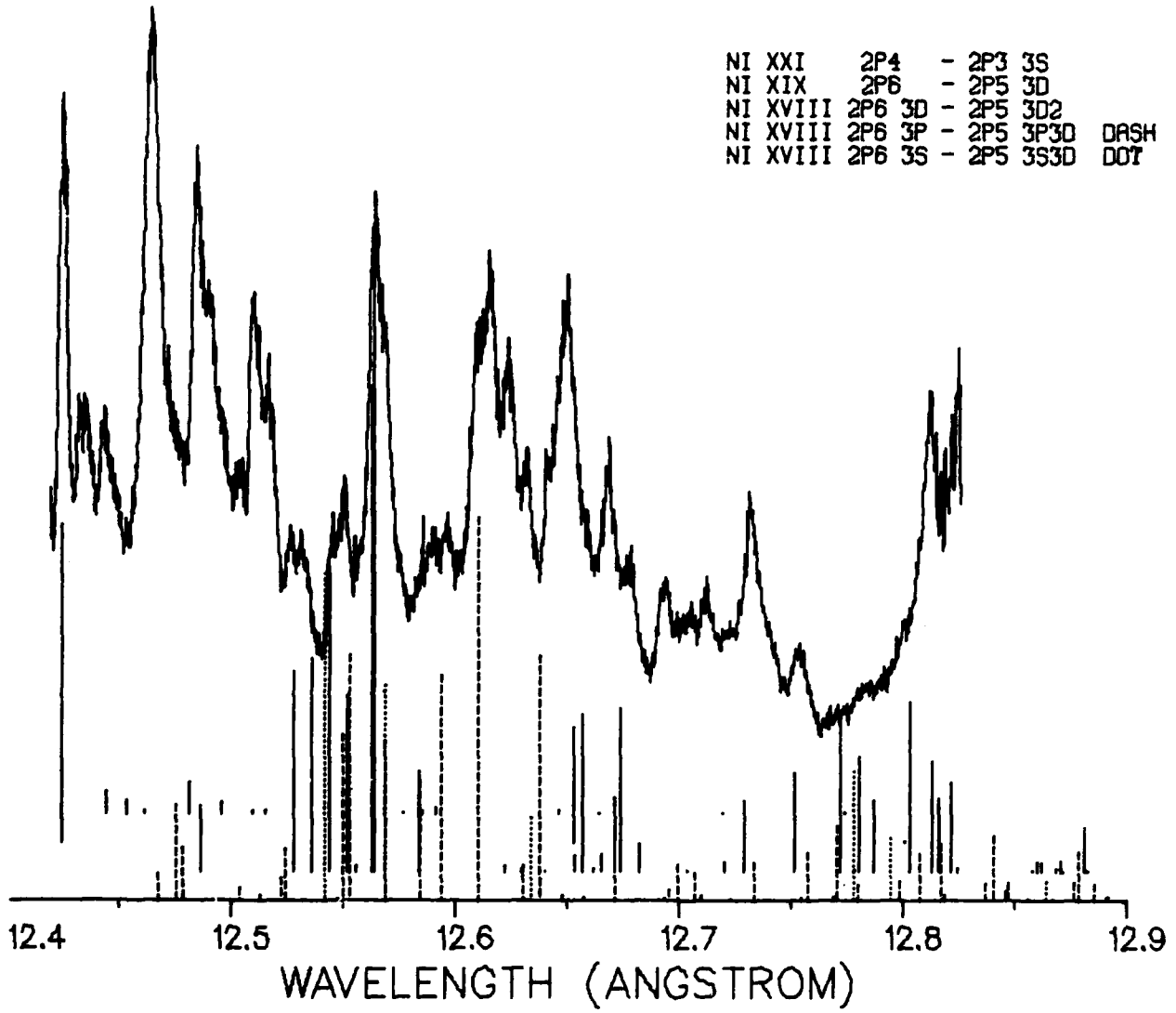

Figure 23. Ni spectrum in the 12.4-12.9 Å region together with at. structure calculations for O-like Ni XXI (top level of theoretical lines), Ne-like Ni XIX (two lines and a weak dot), Na-like Ne XVIII transitions identified by 3d satellites (solid line), 3p satellites (dashed lines), and 3s satellites (dotted lines).

KAP Spectrograph

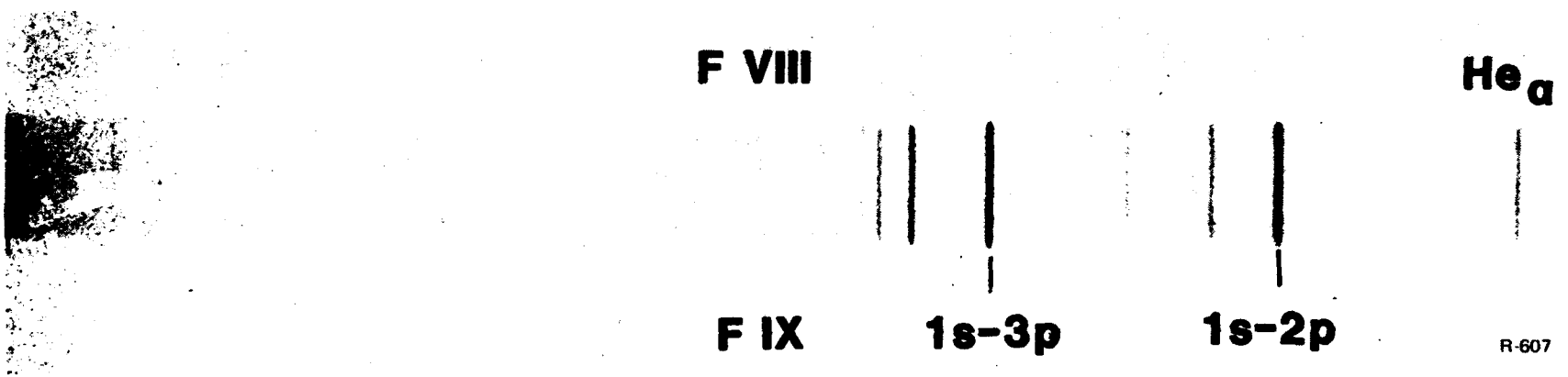

Figure 24. Fluorine spectrogram collected with a curved KAP crystal.

KAP Spectrograph

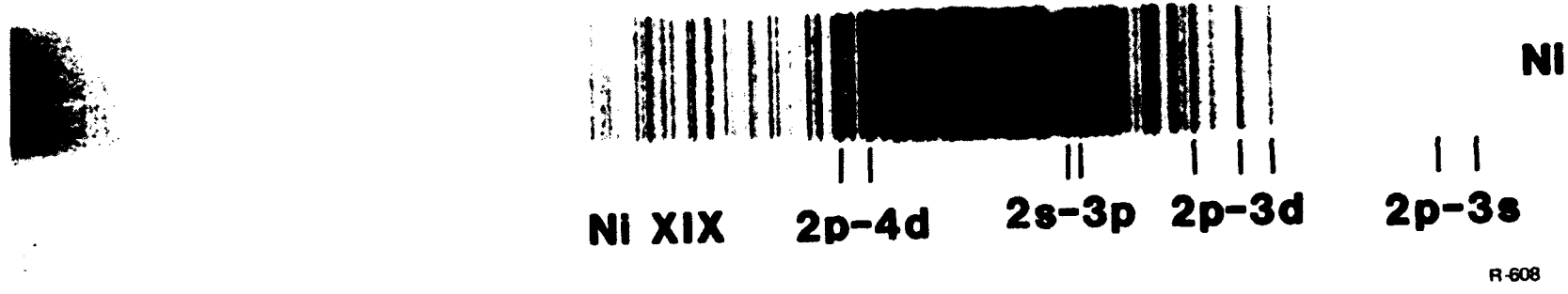

Figure 25. Nickel spectrogram collected with a curved KAP crystal in two shots using green light.

REFERENCES

1. W. Slivinsky, Seminar at N.R.L. held July 27, 1982. Private communications with A. Toor, D. Matthews, P. Hagelstein of Lawrence National Laboratories.

2. P.L. Hagelstein, Physics of Short Wavelength Laser Design, UCRL - 53100, Jan. 1981.

3. J.D. Garcia and J.E. Mack, J.O.S.A. 55, 654 (1965).

4. A.M. Ermolaev, M. Jones and K.J.H. Phillips, Astrophys. Letter. 12 53-56 (1972).

5. H. Gordon, M.G. Hobby, N.J. Peacock, J. Phys B13, 1985-1999 (1980).

6. U. Feldman, G.A. Doschek, R.D. Cowan, and L. Cohen, J.O.S.A. 63, 1445-1453 (1973).

7. V.A. Boiko, S.A. Pikuz, A.S. Safronova, and A. Ya. Fayanov, Opt. Spectrosc. 44, 498-499 (1978).

8. N. Spector, A. Zigler, H. Zmora, J.L. Schwob, J.O.S.A. 70, 857-861 (1980).

9. V.A. Boiko, S.A. Pikuz, U.I. Safronova, A.Ya. Faenov, J. Phys. B10, 1253-1263 (1977).

10. E.V. Aglitskii, V.A. Boiko, S.A. Pikuz, and A.Ya. Faenov, Sov. J. Quant. Electron. 4, 956-960 (1975).

11. S. Goldsmith, U.Feldman, L.Oren, and L.Cohen, Astrophys, J. 174, 209-214 (1972).

12. B. Edlen, Physica Scripta 19, 255-257 (1979).

13. U.I. Safronova, J. Quant, Spectrosc, Radiat. Transfer. 1975.

14. R.R. Whitlock, Condensed Matter Physics Branch, N.R.L. wrote the XTLFILM program.

15. L.N. Koppel, "X-ray Calibration of films", SB-5 and RAR 2492 in the 0.18-0.93 keV Region, TR-112-08-02, March 1982.

16. R.W. Hayes and B.J. Kent, J. Phys E: Sci Instrum. 14, 688-692 (1981). Also private communication with B. J. Kent.

17. P.G. Burkhalter, D.B. Brown and M. Gersten, J. Appl. Phys. 52, 4379-4386 (1981).

18. A.J. Burek, D.M. Barrus and R.L. Blake, Astrophys. J. 191, 533-543, (1974).

19. R.D. Cowan, J.O.S.A. 58, 808-818 (1968): R.D. Cowan and D.C. Griffin, J.O.S.A. 66, 1010-1014 (1976).

20. F.E. Irons, R.W.P. McWhirter, N.J. Peacock, J. Phys. B5, 1975-1978 (1972).

21. P.G. Burkhalter, L. Cohen, R.D. Cowan, and U. Feldman, J.O.S.A. 69, 1133-1139 (1979).

22. U. Feldman, G.A. Doschek, D.J. Nagel, W.E. Bering, and R.D. Cowan, Astrophys. J. 187, 417-420 (1974).

23. M. Swartz, S. Kastner, E. Rothe and W. Neupert, J. Phys. B 4 1747-1768 (1971).

24. V.A. Boiko, A. Ya. Faenov, S.A. Pikuz, J. Quant, Spectrosc. Radiat. Transfer 19, 11-50 (1978).

25. D.L. McKenzie, P.B. Landecker, R.M. Broussard, H.R. Rugge, R.M. Young, U. Feldman and G.A. Doschek, Astrophys. J. 241, 409-416 (1980).

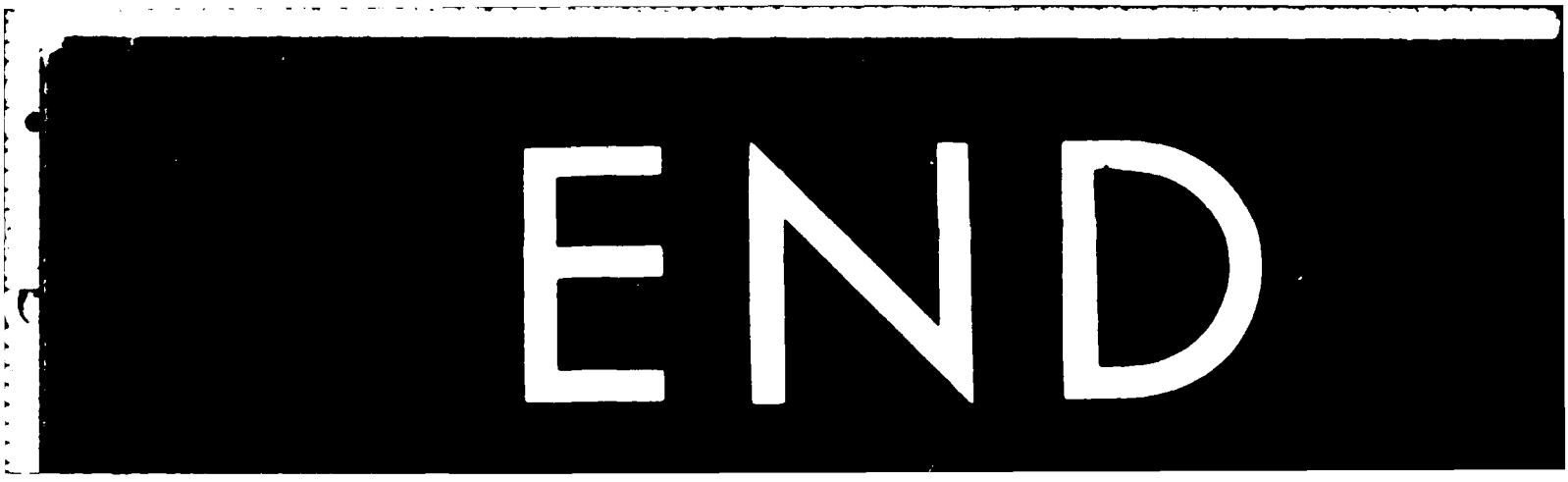
END